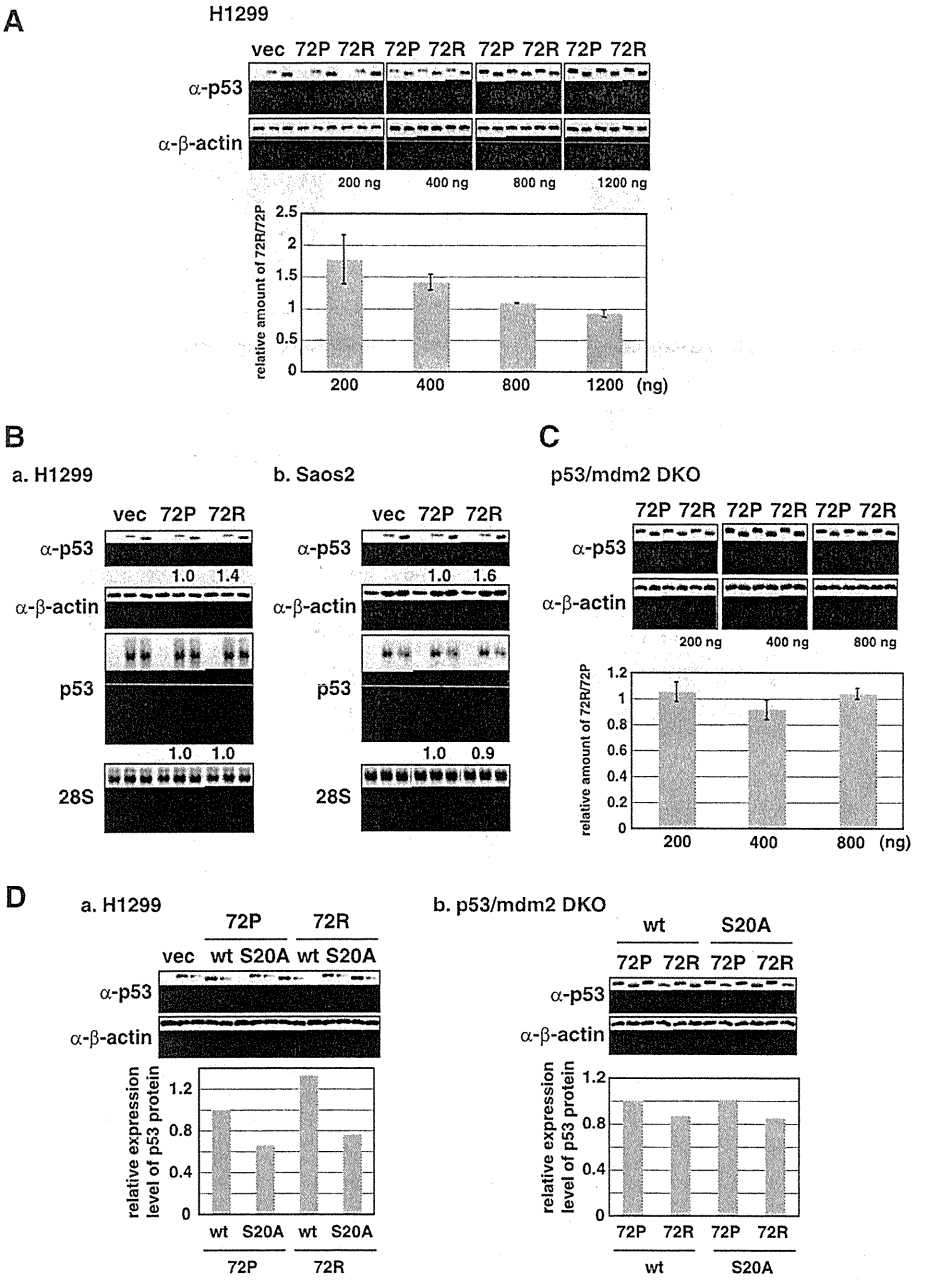

FIGURE 3. **Expression level of p53-72R protein is higher than p53-72P protein.** *A,* indicated amounts of pMX-p53-72P or -72R expression plasmids were introduced into H1299 cells (4.4×10^5 cells/10-cm dish). Cells were harvested 27 h post-transfection and analyzed by Western blotting. Experiments were performed in triplicate, and representative images are shown. The levels of p53 and β-actin were quantified using Image J software, and p53 levels were normalized by β-actin levels. The mean ± S.D. of relative p53-72R/p53-72P levels was calculated and is shown in the *bottom column. vec,* vector. *B,* p53 protein and mRNA levels were analyzed by Western and Northern blotting. The levels of p53 protein (normalized by β-actin levels) and mRNA (normalized by 28 S levels) were quantified using Image J software. *Panel a,* pMX-p53-72P or -72R (0.2 μg) was introduced into H1299 (4.4×10^5 cells/10-cm dish). Cells were harvested 27 h post-transfection. *Panel b,* pMX-p53-72P or -72R (0.9 μg) was introduced into Saos2 cells (4.4×10^6 cells/10-cm dish). Cells were harvested 24 h post-transfection. *C,* indicated amounts of pMX-p53-72P or -72R expression plasmids were introduced into *p53/mdm2* DKO (4.4×10^5 cells/10-cm dish) and analyzed as in *A. D,* expression plasmids (cloned in pMX vector) of wild-type or mutant (S20A) p53-72P or -72R were introduced into H1299 (in *panel a*, 4.4×10^5 cells/10-cm dish, 500 ng transfected) or *p53/mdm2* DKO (in *panel b*, 4.4×10^5 cells/10-cm dish, 200 ng transfected) cells. Cells were harvested 21 h (*panel a*) or 27 h (*panel b*) post-transfection. Experiments were performed in duplicate, and the mean values of relative p53-72P and -72R levels are presented.

shown in Fig. 4*A*, although p53-72P was efficiently degraded under the conditions tested, p53-72R was resistant to degradation. We further analyzed the ubiquitination of both variants by Mdm2. His-tagged ubiquitin was co-expressed with p53 and Mdm2 in H1299 cells. Cell lysates were prepared, and p53 was immunoprecipitated by anti-p53 antibody. Immunoprecipitates were analyzed by Western blotting using anti-His tag antibody. As shown in Fig. 4*B*, it was shown that His-tagged ubiquitinated p53 was more prominent in p53-72P than p53-72R. We also performed a nickel pulldown assay under denaturing conditions to purify His-tagged ubiquitinated proteins. The samples were then analyzed by Western blotting using anti-p53

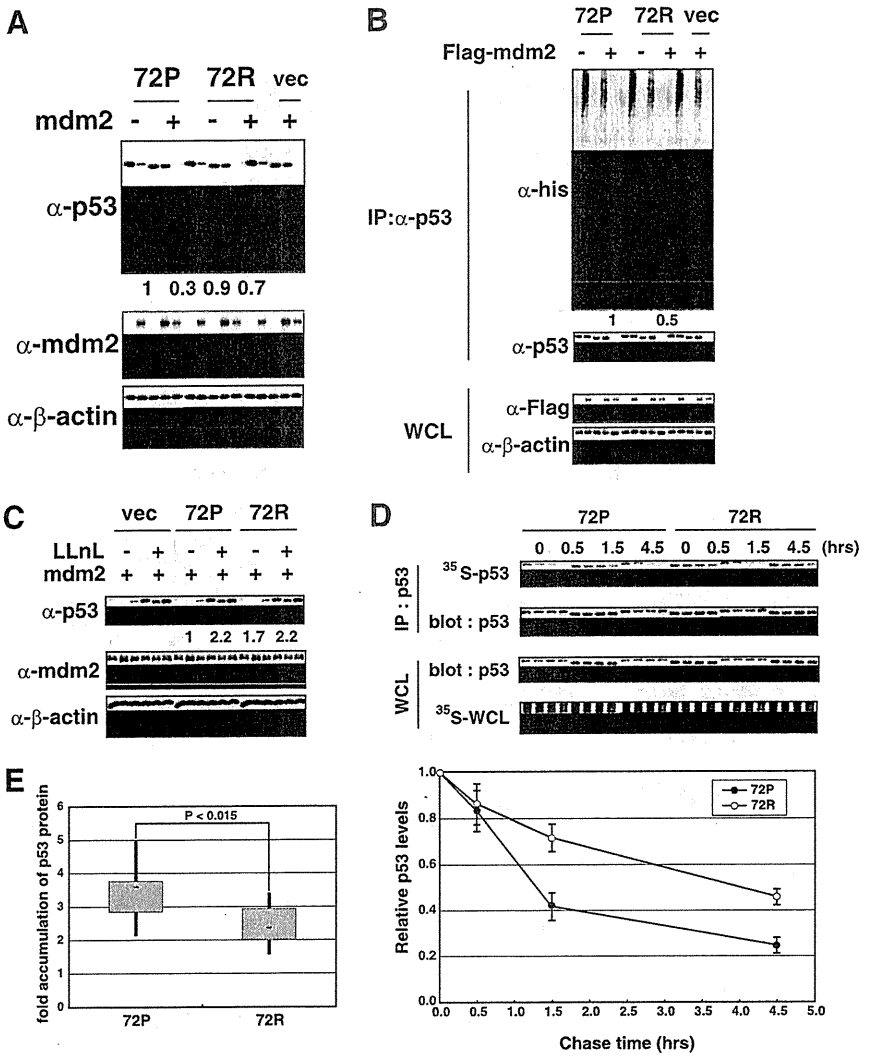

FIGURE 4. **Degradation of p53-72P by Mdm2 is accelerated compared with p53-72R.** *A*, pcDNA3-p53-72P or -72R together with N-terminally c-Myc-tagged Mdm2 (pCMV-Myc-Mdm2; Mdm2 expressed from a CMV promoter) or control empty vector were introduced into H1299 cells (4.4×10^5 cells/10-cm dish) and analyzed by Western blotting. 0.44 μg of p53 and 4 μg of Mdm2 were transfected. Cells were harvested 21 h post-transfection. Levels of p53 (normalized by β-actin) were quantified and are shown *below* the panels. *B*, pcDNA3-p53-72P or -72R (0.35 μg) together with His_6-tagged ubiquitin (2.2 μg) and N-terminally FLAG-tagged Mdm2 (pSG-FLAG-Hdm2, 1.42 μg) or control empty vector (*vec*) (1.42 μg) were introduced into H1299 cells (6×10^5 cells/10-cm dish), and cells were harvested 27 h post-transfection. To detect ubiquitinated p53 efficiently, Mdm2 was expressed at a low level using expression plasmid pSG-F-Hdm2 (Hdm2 is under the control of SV40 promoter, which is much weaker than CMV promoter). p53 was immunoprecipitated (*IP*) with anti-p53 polyclonal antibody (FL393), and immunoprecipitated samples and whole cell lysates (*WCL*) were analyzed by Western blotting. Western blot analyses of immunoprecipitates were performed with the anti-His antibody to detect ubiquitinated p53 (*upper panel*) or with FL393 antibody to detect nonubiquitinated p53 (*lower panel*). Levels of ubiquitinated p53 (normalized by nonubiquitinated p53) were quantified and are shown *below* the panels. *C*, pMX-p53-72P or -72R (0.5 μg) together with pCMV-Myc-Mdm2 (4.5 μg) or control empty vector (4.5 μg) were introduced into H1299 cells (4.4×10^5 cells/10-cm dish). Where indicated, cells were treated with LLnL (50 μM) 16 h post-transfection. Cells were harvested 21 h post-transfection and analyzed by Western blotting. Experiments were performed in triplicate, and representative images are shown. Levels of p53 were quantified (normalized by β-actin) and the relative p53-72P and -72R levels are shown *below* the panel. *D*, pcDNA3-p53-72P or -72R (0.4 μg) together with pCMV-Myc-Mdm2 (3.6 μg) were introduced into H1299 cells (4×10^5 cells/10-cm dish). Cells were pulse-labeled 20 h post-transfection for 30 min and then cultured in chase medium for 1.5 h. Following incubation, cells were harvested at the indicated time points. p53 was immunoprecipitated, and the levels of labeled p53 were detected by autoradiography. Total p53 protein levels were analyzed by Western blotting. Experiments were performed in triplicate, and representative images are shown. Levels of p53 were quantified (normalized by total p53) and the relative p53-72P and -72R levels are shown *below* the panel. *E*, immortalized peripheral lymphocytes from healthy donors were subjected to LLnL treatment. Cells derived from 10 homozygotes each for p53-72P and -72R were subjected to analysis. Each sample was run in triplicate and analyzed by Western blotting (supplemental Fig. S3). Quantification was performed using Image J software. Fold accumulation of p53 protein after LLnL treatment was calculated for each sample and shown as a *box plot*.

antibody to detect the amount of His-tagged ubiquitinated p53s. Again, ubiqitination was more prominent in p53-72P than p53-72R (supplemental Fig. S2).

To further test whether the variants differ in degradation levels mediated by the proteasome pathway, we treated cells co-expressing Mdm2 and p53-72R or -72P with LLnL, a proteasome inhibitor. As shown in Fig. 4*C*, the p53-72P level was significantly increased by LLnL treatment compared with p53-72R, showing that p53-72P is more susceptible to degradation by the proteasome pathway. In addition, both variants were expressed at similar levels after LLnL treatment, supporting the idea that differences in the expression levels of both variant

TABLE 1
Over-representation of p53–72P homozygotes in lung cancer cases with gains of the *mdm2* gene in their tumors

p53 genotype	No. of cases: MDM2 normal	MDM2 gain[a]	Odd ratio (95% confidence interval)	*p* value by Fisher's exact test
	%	%		
R/R + R/P	48 (94)	19 (79)	Reference	
P/P	3 (6)	5 (21)	4.21 (0.94–22.2)	0.101

[a] Copy number ratio >1.25 in tumors by array comparative genomic hybridization analysis using MCG Cancer array-800.

proteins were the result of proteasomal degradation. We also performed [^{35}S]methionine pulse-chase experiments to determine the half-lives of p53 variant proteins. Cells co-expressing Mdm2 and p53-72R or -72P were pulse-labeled, and p53 protein levels were monitored for 4.5 h. As shown in Fig. 4*D*, the half-life of p53-72R was significantly longer than p53-72P, demonstrating that p53-72R is more resistant to Mdm2-mediated degradation.

We next utilized peripheral lymphocytes immortalized using Epstein-Barr virus to analyze the degradation of endogenously expressed p53 proteins. We selected 10 cells each that were homozygous for p53-72P or -72R. To minimize the difference between cell lines, they were also selected based on the criteria that they were derived from healthy donors who were Japanese, male, nonsmoking, and aged 30–50 years old. As shown in supplemental Fig. S3 and Fig. 4*E*, when cells were treated with LLnL, accumulation of p53 protein was more pronounced in cells with p53-72P, confirming the result obtained for exogenously expressed p53 proteins. Collectively, it was shown that ubiquitination by Mdm2 and subsequent degradation is more enhanced in p53-72P than -72R.

Cancer Patients Carrying p53-72P Are Over-represented in Patients with Gain in the mdm2 Gene—The nature of p53-72P being more sensitive to degradation by Mdm2 than p53-72R raises the possibility that homozygotes for the p53-72P allele are more susceptible to developing cancer by up-regulation of Mdm2 expression. We therefore analyzed the copy number of the *mdm2* gene in tumors in combination with genotypes for the p53 polymorphism at codon 72 in the germ line. Seventy five lung cancer cases, consisting of 39 adenocarcinomas, 2 bronchioalveolar carcinomas, 25 squamous cell carcinomas, 2 small cell lung carcinomas, 7 large cell neuroendocrine carcinoma cases, that were available for information both on p53 genotypes in their peripheral blood cells and the *mdm2* gene copy numbers in their tumor cells were subjected to analysis (Table 1). These cases were selected from a Japanese population of lung cancer cases that showed a frequency of the p53-72P allele higher than control individuals in a previous case-control study based on the criterion that information on the *mdm2* gene copy numbers in their tumor was available (19). In fact, the frequency of the p53-72P allele in these 75 cases (*i.e.* 0.41) was higher than that of controls (*i.e.* 0.33), although the difference did not reach statistical significance ($p = 0.070$ by Fisher's exact test). Among the 75 cases, 24 (32%) showed gain of the *mdm2* gene (ratio of test signal/reference signal >1.25) in their tumors. The fraction of p53-72P homozygotes was notably higher in patients with *mdm2* gains in their tumors than without (21 *versus* 6%, $p = 0.101$ by Fisher's exact test). Although further study is required with more test cases, these data suggest that p53-72P individuals develop lung cancer at a higher frequency upon increase of the *mdm2* gene copy number and support our results showing that p53-72P is more susceptible to Mdm2-mediated degradation.

Phosphorylation of Ser-6 Is More Enhanced in p53-72R than -72P under Basal and Damaged Conditions—Ser-6, Ser-15. and Thr-18 are the phosphorylation sites within the N-terminal transactivation domain that are conserved among vertebrates. Phosphorylation of Ser-15 and Thr-18 plays important roles in the regulation of p53 activity; however, although it has been reported that Ser-6 is phosphorylated under damaged or basal conditions, the biological significance of Ser-6 phosphorylation remains elusive (6). Because we found that Ser-6 is strongly phosphorylated in p53-72R compared with p53-72P in Saos2 cells (Fig. 2), we further analyzed under which conditions Ser-6 is phosphorylated. As shown in Fig. 5*A*, upon γ-ray irradiation, the Ser-6 phosphorylation level is increased, and p53-72R is phosphorylated at a higher level than p53-72P in Saos2 cells. In this experiment, the difference in Ser-6 phosphorylation without DNA damage was also confirmed. Under the same conditions, phosphorylation of Ser-15 was induced upon γ-ray irradiation, but no difference was detected between variants with or without γ-ray irradiation. To further analyze p53 phosphorylation under damaged conditions, we obtained cell lines stably expressing both p53s in HCT116 p53(−/−) cells. As shown in supplemental Fig. S4*A*, both cell lines expressed p53-72R or -72P at similar levels and induced p21 upon DNA damage, showing a normal p53 response in these cell lines. Using these cell lines, phosphorylation of Ser-6 under basal conditions and upon DNA damage was analyzed. As shown in Fig. 5*B* and supplemental Fig. S4, *B* and *C* upon γ-ray or UV irradiation, adriamycin or 5-fluorouracil treatment resulted in increased Ser-6 phosphorylation, and under all conditions, p53-72R showed elevated phosphorylation levels compared with p53-72P. Again, phosphorylation of Ser-15 was induced upon γ-ray irradiation, but no difference was detected between variants (Fig. 5*B*).

Phosphorylation of Ser-6 Is Required for p53 Transactivation under Basal Conditions and upon Activation of TGF-β Signaling—To analyze the biological function of Ser-6 phosphorylation, we constructed p53 mutants carrying Ser to Ala conversions at codon 6. Wild-type as well as mutant p53s were expressed in H1299 cells, and the induction of representative p53 target gene products (p21, Bax, PIG-3, and Mdm2) were analyzed by Western blotting. As shown in Fig. 5*C*, all four p53 target gene products were induced by wild-type p53 as expected. Interestingly, wild-type p53 induced p21 more effectively than S6A mutant, demonstrating the involvement of Ser-6 phosphorylation in p21 induction. In addition, as shown in Fig. 5*D*, p53-72R induced p21 more strongly than p53-72P, likely reflecting the difference in Ser-6 phosphorylation levels between proteins. The elevated expression of p21 in p53-72R-expressing cells was also demonstrated in HCT116 p53(−/−) cells stably expressing p53-72P or -72R and in immortalized human peripheral lymphocytes (supplemental Figs. S4*A* and S5*A*).

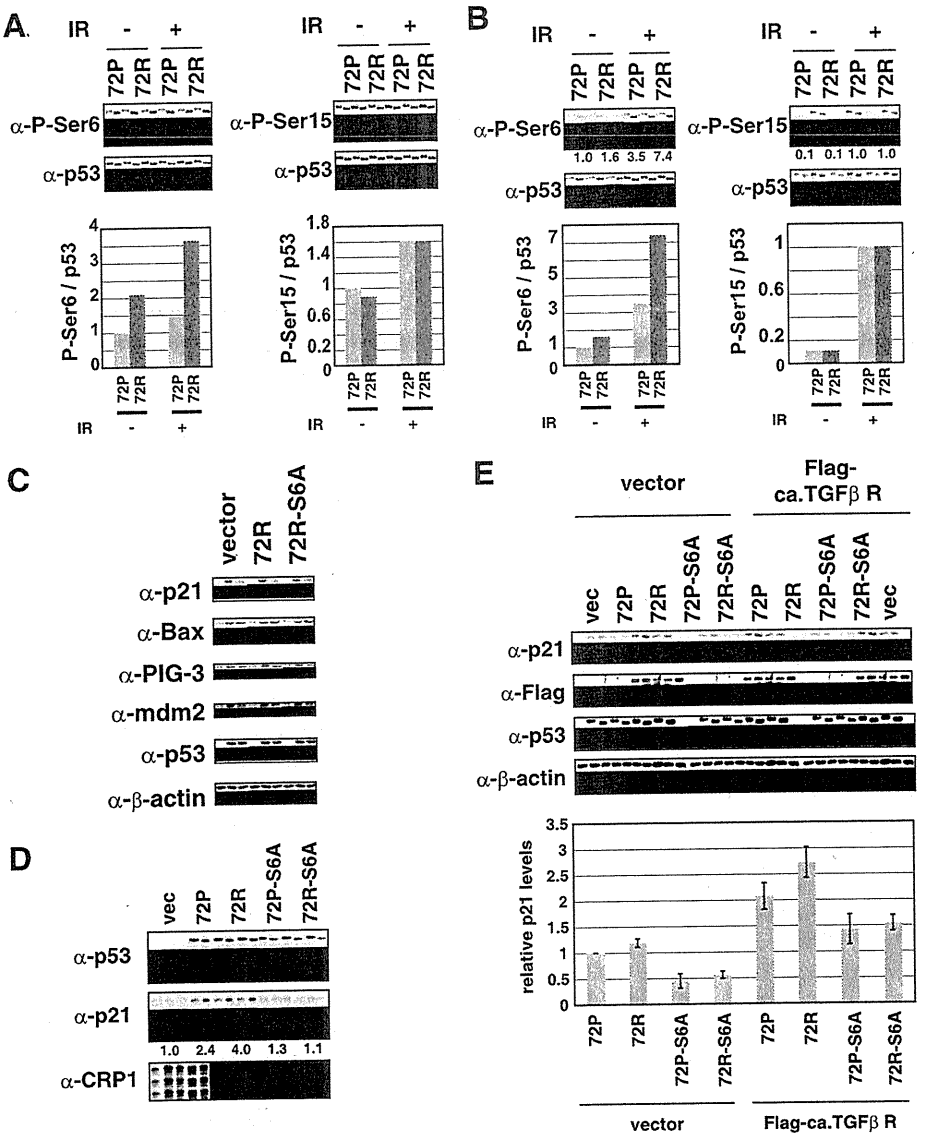

FIGURE 5. **Phosphorylation of p53 at Ser-6 was enhanced in p53-72R compared with -72P, and p53-dependent p21 expression was enhanced in cells expressing p53-72R.** *A*, phosphorylation of p53 at Ser-6 and Ser-15 in Saos2 cells expressing p53-72P or -72R was analyzed by Western blotting. Cells (2.2×10^6 cells/10-cm dish) were transfected with pMX-p53-72P or -72R, treated with γ-ray (20 gray) 24 h post-transfection, and harvested 50 h post-transfection. As in Fig. 2, p53 proteins were immunoprecipitated and analyzed using anti-phospho-Ser-6 p53 antibody (*upper panel*) and anti-p53 antibody (*lower panel*). Levels of phospho-Ser-15 are shown for comparison. To detect phospho-Ser-15 and total p53 in *right panels*, whole cell lysates were analyzed by Western blotting. Relative phosphorylation levels (normalized by total p53 levels) are shown *below* the panels. *B*, HCT116 p53(−/−) cells stably expressing p53-72P or -72R (6.7×10^6 cells/10-cm dish) were treated with γ-ray (20 gray), and cells were harvested 2 h post-irradiation. Levels of phospho-Ser-6 and -15 were analyzed as in *A*. *C*, H1299 cells (4×10^5 cells/10-cm dish) were transfected with pMX-p53-72R or 72R-S6A mutant (0.3 μg) together with pcDNA3 (2.7 μg). Cells were harvested 26 h post-transfection, and analyzed by Western blotting. *D*, wild-type or mutant (S6A) pMX-p53-72P or -72R (1.63 μg) was introduced into H1299 cells (2.4×10^6 cells/10-cm dish), and cells were harvested 29 h post-transfection. Expression of p53, p21, and cytoskeletal CRP1 (as a loading control) was analyzed by Western blotting. The experiment was performed with p53-72P and -72R expressed at similar levels. The levels of p21 and 23-kDa CRP1 were quantified using Image J software, and p21 levels were normalized by CRP1 levels. *E*, H1299 cells (2.4×10^6 cells/10-cm dish) were transfected with pMX-p53-72P or 72R (1.63 μg) and ca. TGF-βR (6.54 μg). Cells were harvested 29 h post-transfection. Expression of ca. TGF-βR was detected by anti-FLAG antibody. Experiments were performed in triplicate, and representative images are shown. The levels of p21 (normalized by β-actin) were quantified using Image J software. The mean ± S.D. of p21 levels was calculated and is shown in the *bottom column*.

It has been reported that the activation of MAPK promotes the phosphorylation of p53 at Ser-6 and Ser-9 (25). Phosphorylation at these sites facilitates the interaction of p53 with activated Smad2 or Smad3 and the subsequent recruitment of p53-Smad2/3 complexes to TGF-β-responsive target promoters (25). As shown in supplemental Fig. S4*D*, we also have confirmed MAPK-dependent phosphorylation of p53 at Ser-6. It has also been shown using H1299 cells that the expression of p53 with amino acid conversions from Ser to Ala at codon 6 or 9 impaired the ability of p53 to enhance TGF-β-mediated expression of the p21 gene (25). Because we detected a significant difference in Ser-6 phosphorylation between the variants, we analyzed whether TGF-β-mediated expression of the p21 gene differs between them. We analyzed TGF-β-dependent up-regulation of p21 by introducing constitutively active TGF-β receptor I (ca. TGF-βR) with p53 variants. It was confirmed

that introduction of ca. TGF-βR results in activation of the TGF-β pathway in H1299 cells, as judged from Smad2 phosphorylation (supplemental Fig. S5*B*). As shown in supplemental Fig. S5*B* and Fig. 5*E*, without TGF-β signaling, p53-72R induced p21 more efficiently than p53-72P, confirming the results shown in Fig. 5*D*. When ca. TGF-βR was co-transfected with p53s, TGF-β-dependent up-regulation of p21 was observed, and this induction was significantly stronger in cells expressing p53-72R. Enhanced induction efficiency of p21 in p53-72R-expressing cells with or without ca. TGF-βR was also confirmed by quantitative real time PCR (supplemental Fig. S5*C*). The difference between variants was abolished when Ser to Ala conversions were introduced at Ser-6, showing that the difference in p21 induction was brought about from differences in Ser-6 phosphorylation levels (Fig. 5*E*). Collectively, these results indicate that Ser-6 phosphorylation is important for p53 transactivation activity under basal conditions and upon activation of TGF-β signaling, and enhanced Ser-6 phosphorylation in p53-72R results in stronger induction of p21.

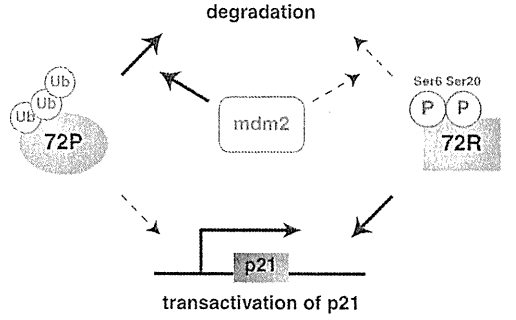

FIGURE 6. **Common polymorphism of p53 affects phosphorylation and degradation of p53 protein.** Phosphorylation of Ser-6 and -20 is enhanced in p53-72R compared with p53-72P. Difference in protein structure and phosphorylation of Ser-20 affects Mdm2-mediated degradation of p53 protein, whereas phosphorylation of Ser-6 affects transactivation ability of p53 protein.

DISCUSSION

The polymorphism of p53 at codon 72 is unique to humans and is very common. For example, 44% of Japanese are homozygous for p53-72R and 11% are homozygous for p53-72P (19). Cancer susceptibility and clinical outcome differ among individuals having the two variants; therefore, the impact of understanding the molecular basis for the difference between p53-72P and -72R is huge. Recently, using chimeric p53 protein containing N-terminal mouse p53 (amino acids 1–34) and human p53 (amino acids 32–393), it was shown that codon 72 polymorphism-specific effects of human p53 require N-terminal 31 amino acids of human p53 (26). In addition, we found that p53-72R and -72P proteins differ in structure, especially in the N-terminal region, by partial proteolytic digestion of the proteins. We speculated that differences in the protein structure may change the affinity of p53 variants with kinases that modify p53, especially in the N-terminal region, and we found that the variants differ in phosphorylation levels at Ser-6 and -20. We actually found that strength of association with Chk2 kinase differs between p53-72P and p53-72R (supplemental Fig. S6). We do not know the precise mechanism of the differential association of the variants with Chk2, and it is an interesting issue to clarify in future research.

It has been reported that p53 phosphorylated at Ser-20 escapes from degradation by Mdm2, leading to stabilization of the protein (6), whereas phosphorylation of Ser-6 is required for TGF-β-dependent induction of p21 and p15INK4b (25). We found that phosphorylation of these sites is enhanced in p53-72R, and consequently, the two p53 polymorphic variants differ in the stabilization of proteins and TGF-β-dependent and -independent induction of p21, both of which are important for the tumor-suppressive function of p53 (Fig. 6).

In this study, we have shown for the first time that the *mdm2* gene gain in tumors is more frequent in lung cancer cases homozygous for the p53-72P allele than with other genotypes. Although this association should be further validated in other sets of lung cancer cases, the present result demonstrates the possibility that p53-72P homozygotes develop lung cancer at a higher frequency upon gain of the *mdm2* gene and supports our data showing that p53-72P is more susceptible to Mdm2-mediated degradation. It will be interesting to determine whether such an association is also observed in patients with other types of cancer.

Previously, it was shown that the expression of p21 mRNA was altered by p53 codon 72 polymorphism, and the Pro allele variant was associated with decreased p21 mRNA levels compared with Arg allele (27). In this study, we have also shown that p21 expression was decreased in p53-72P compared with -72R and was dependent on p53 Ser-6 phosphorylation. The physiological relevance of Ser-6 phosphorylation remains unknown; however, it was shown recently to be required for TGF-β signaling. TGF-β is a potent growth inhibitor with tumor suppressing activity, and TGF-β-mediated growth suppression is mediated by p53 (28). TGF-β cooperates with p53 to induce p21, and this induction requires p53 to be phosphorylated at N-terminal Ser residues, including Ser-6 (25). We have shown that p53-72P was less phosphorylated at Ser-6 compared with p53-72R under all conditions studied, and TGF-β-dependent and -independent induction of p21 was attenuated in p53-72P-expressing cells. Previously, we have shown that phosphorylation of Ser-6 does not affect binding of p53 to p21 promoter (8). Therefore, Ser-6 may affect other aspects of p21 promoter activation, such as cofactor recruitment to the promoters.

The results shown in this study collectively reveal a novel difference in p53 polymorphic variants at codon 72. Although several molecular mechanisms to explain the difference in tumor suppression function of the variants have been reported, our results also reveal a novel difference in the variants through differences in protein structure and phosphorylation levels at Ser-6 and -20. Understanding the molecular mechanism leading to differences in the tumor suppression potential of the two variants is very important for cancer prevention and therapy. Our results may provide basic knowledge to develop novel cancer therapy or prevention strategies on the basis of the genotype of p53.

Acknowledgments—We thank Dr. Teruhiko Yoshida for providing immortalized peripheral lymphocytes. We also thank Dr. Yasumichi Inoue for providing pcDNA4-HisMax-Chk2 plasmid.

REFERENCES

1. Vogelstein, B., Lane, D., and Levine, A. J. (2000) *Nature* **408**, 307–310
2. Vousden, K. H., and Lu, X. (2002) *Nat. Rev. Cancer* **2**, 594–604
3. Braithwaite, A. W., and Prives, C. L. (2006) *Cell Death Differ.* **13**, 877–880
4. Prives, C. (1998) *Cell* **95**, 5–8
5. Xu, Y. (2003) *Cell Death Differ.* **10**, 400–403
6. Bode, A. M., and Dong, Z. (2004) *Nat. Rev. Cancer* **4**, 793–805
7. Oda, K., Arakawa, H., Tanaka, T., Matsuda, K., Tanikawa, C., Mori, T., Nishimori, H., Tamai, K., Tokino, T., Nakamura, Y., and Taya, Y. (2000) *Cell* **102**, 849–862
8. Kawase, T., Ichikawa, H., Ohta, T., Nozaki, N., Tashiro, F., Ohki, R., and Taya, Y. (2008) *Oncogene* **27**, 3797–3810
9. Kawase, T., Ohki, R., Shibata, T., Tsutsumi, S., Kamimura, N., Inazawa, J., Ohta, T., Ichikawa, H., Aburatani, H., Tashiro, F., and Taya, Y. (2009) *Cell* **136**, 535–550
10. Unger, T., Sionov, R. V., Moallem, E., Yee, C. L., Howley, P. M., Oren, M., and Haupt, Y. (1999) *Oncogene* **18**, 3205–3212
11. Toledo, F., and Wahl, G. M. (2006) *Nat. Rev. Cancer* **6**, 909–923
12. Zilfou, J. T., Hoffman, W. H., Sank, M., George, D. L., and Murphy, M. (2001) *Mol. Cell. Biol.* **21**, 3974–3985
13. Bergamaschi, D., Samuels, Y., Sullivan, A., Zvelebil, M., Breyssens, H., Bisso, A., Del Sal, G., Syed, N., Smith, P., Gasco, M., Crook, T., and Lu, X. (2006) *Nat. Genet.* **38**, 1133–1141
14. Harris, N., Brill, E., Shohat, O., Prokocimer, M., Wolf, D., Arai, N., and Rotter, V. (1986) *Mol. Cell. Biol.* **6**, 4650–4656
15. Murphy, M. E. (2006) *Cell Death Differ.* **13**, 916–920
16. Matlashewski, G. J., Tuck, S., Pim, D., Lamb, P., Schneider, J., and Crawford, L. V. (1987) *Mol. Cell. Biol.* **7**, 961–963
17. Soussi, T., and Wiman, K. G. (2007) *Cancer Cell* **12**, 303–312
18. Fan, R., Wu, M. T., Miller, D., Wain, J. C., Kelsey, K. T., Wiencke, J. K., and Christiani, D. C. (2000) *Cancer Epidemiol. Biomarkers Prev.* **9**, 1037–1042
19. Sakiyama, T., Kohno, T., Mimaki, S., Ohta, T., Yanagitani, N., Sobue, T., Kunitoh, H., Saito, R., Shimizu, K., Hirama, C., Kimura, J., Maeno, G., Hirose, H., Eguchi, T., Saito, D., Ohki, M., and Yokota, J. (2005) *Int. J. Cancer* **114**, 730–737
20. Boldrini, L., Gisfredi, S., Ursino, S., Lucchi, M., Greco, G., Mussi, A., and Fontanini, G. (2008) *Oncol. Rep.* **19**, 771–773
21. Tommiska, J., Eerola, H., Heinonen, M., Salonen, L., Kaare, M., Tallila, J., Ristimäki, A., von Smitten, K., Aittomäki, K., Heikkilä, P., Blomqvist, C., and Nevanlinna, H. (2005) *Clin. Cancer Res.* **11**, 5098–5103
22. Ohki, R., Kawase, T., Ohta, T., Ichikawa, H., and Taya, Y. (2007) *Cancer Sci.* **98**, 189–200
23. Okamoto, K., Kashima, K., Pereg, Y., Ishida, M., Yamazaki, S., Nota, A., Teunisse, A., Migliorini, D., Kitabayashi, I., Marine, J. C., Prives, C., Shiloh, Y., Jochemsen, A. G., and Taya, Y. (2005) *Mol. Cell. Biol.* **25**, 9608–9620
24. Shibata, T., Uryu, S., Kokubu, A., Hosoda, F., Ohki, M., Sakiyama, T., Matsuno, Y., Tsuchiya, R., Kanai, Y., Kondo, T., Imoto, I., Inazawa, J., and Hirohashi, S. (2005) *Clin. Cancer Res.* **11**, 6177–6185
25. Cordenonsi, M., Montagner, M., Adorno, M., Zacchigna, L., Martello, G., Mamidi, A., Soligo, S., Dupont, S., and Piccolo, S. (2007) *Science* **315**, 840–843
26. Phang, B. H., and Sabapathy, K. (2007) *Oncogene* **26**, 2964–2974
27. Su, L., Sai, Y., Fan, R., Thurston, S. W., Miller, D. P., Zhou, W., Wain, J. C., Lynch, T. J., Liu, G., and Christiani, D. C. (2003) *Lung Cancer* **40**, 259–266
28. Cordenonsi, M., Dupont, S., Maretto, S., Insinga, A., Imbriano, C., and Piccolo, S. (2003) *Cell* **113**, 301–314

blood

2011 118: 1600-1609
Prepublished online May 25, 2011;
doi:10.1182/blood-2011-01-329433

Missense mutations in *PML-RARA* are critical for the lack of responsiveness to arsenic trioxide treatment

Emi Goto, Akihiro Tomita, Fumihiko Hayakawa, Akihide Atsumi, Hitoshi Kiyoi and Tomoki Naoe

Blood (print ISSN 0006-4971, online ISSN 1528-0020), is published weekly by the American Society of Hematology, 2021 L St, NW, Suite 900, Washington DC 20036.

Missense mutations in *PML-RARA* are critical for the lack of responsiveness to arsenic trioxide treatment

Emi Goto,[1] Akihiro Tomita,[1] Fumihiko Hayakawa,[1] Akihide Atsumi,[1] Hitoshi Kiyoi,[1] and Tomoki Naoe[1]

[1]Department of Hematology and Oncology, Nagoya University Graduate School of Medicine, Nagoya, Japan

Arsenic trioxide (As_2O_3) is a highly effective treatment for patients with refractory/relapsed acute promyelocytic leukemia (APL), but resistance to As_2O_3 has recently been seen. In the present study, we report the findings that 2 of 15 patients with refractory/relapsed APL treated with As_2O_3 were clinically As_2O_3 resistant. Leukemia cells from these 2 patients harbored missense mutations in promyelocytic leukemia gene–retinoic acid receptor-α gene (*PML-RARA*) transcripts, resulting in amino acid substitutions of A216V and L218P in the PML B2 domain. When wild-type or mutated PML-RARA (PR-WT and PR-B/L-mut, respectively) were overexpressed in HeLa cells, immunoblotting showed SUMOylated and/or oligomerized protein bands in PR-WT but not in PR-B/L-mut after As_2O_3 treatment. Protein-localization analysis indicated that PR-WT in the soluble fraction was transferred to the insoluble fraction after treatment with As_2O_3, but PR-B/L-mut was stably detected in fractions both with and without As_2O_3. Immunofluorescent microscopy analysis showed PR-WT localization as a microgranular pattern in the cytoplasm without As_2O_3 and as a macrogranular pattern with As_2O_3. PR-B/L-mut was diffusely observed in the cytoplasm with and without As_2O_3. Nearly identical localization patterns were observed in patients' primary cells. Therefore, B2 domain mutations may play an important role in aberrant molecular responses to As_2O_3 and may be critical for As_2O_3 resistance in APL. (*Blood.* 2011;118(6):1600-1609)

Introduction

Acute promyelocytic leukemia (APL) is characterized by the reciprocal chromosomal translocation t(15;17)(q22;q21), leading to fusion of the promyelocytic leukemia gene (*PML*) on chromosome 15 and the retinoic acid receptor-α gene (*RARA*) on chromosome 17.[1] *PML-RARA* fusions are detectable in > 95% of patients with APL. In 1985, *all-trans* retinoic acid (ATRA) was introduced for the treatment of APL as a differentiation therapy, and a dramatic improvement in the overall survival of patients with APL has been obtained.[2-4] However, approximately 10%-30% of patients eventually relapse after treatment with combination chemotherapies with ATRA.[5-7]

Arsenic trioxide (As_2O_3) is a critical drug for the treatment of APL and is clinically effective even in ATRA-resistant patients.[8] As_2O_3 is a natural substance that has been used medically for over 2400 years. In the 1970s, a group in China identified As_2O_3 as a component of an anticancer reagent.[9] Over the last 18 years, clinical trials conducted worldwide have demonstrated the efficacy of As_2O_3 for the treatment of relapsed patients with APL.[10,11] Recently, it was also reported that As_2O_3 improves event-free survival and overall survival of adult APL when As_2O_3 is used as a consolidation treatment after obtaining the first remission.[12] Currently, the role of As_2O_3 in frontline therapy is under investigation.[10,13]

Rapid degradation of PML-RARA via targeting of PML has been reported as a molecular mechanism for the effectiveness of As_2O_3.[14] Furthermore, As_2O_3 induces posttranslational modifications of PML-RARA with small ubiquitin-related modifier (SUMO) and ubiquitin, resulting in the transfer of PML-RARA from the soluble fraction to the insoluble nuclear matrix[14] and the degradation of both PML and PML-RARA.[14-17] In addition to the significant clinical effectiveness of As_2O_3 for patients with APL, acquired resistance to As_2O_3 therapy has been recognized in clinical practice.[18] Several studies have indicated that arsenic-resistant NB4 cells in vitro show higher glutathione levels than in parental cells.[19-21] However, the detailed molecular mechanisms of resistance to As_2O_3 remain unclear.

Very recently, 2 studies reported that As_2O_3 binds directly to cysteine residues in zinc fingers located within the RBCC motif that contains 3 cysteine-rich zinc-binding domains, a RING-finger (R), 2 B-box motifs (B1 and B2), and a coiled-coil (CC) domain,[22,23] in PML-RARA and PML.[24,25] An intriguing hypothesis is that impairment of As_2O_3 binding to PML-RARA due to conformational changes may result from genetic mutations and/or abnormal posttranslational modifications. These events may be related to resistance to As_2O_3 therapy.

We report the clinical significance and frequency of As_2O_3 resistance in patients with APL. Fifteen patients with APL were treated with As_2O_3 after combination chemotherapy with ATRA, and 2 patients showed clinical As_2O_3 resistance. Interestingly, in both of these As_2O_3-resistant patients, missense genetic mutations in the *PML-RARA* fusion transcript were observed in the leukemia cells. We demonstrated that the mutations, which were located in the PML RBCC region, were critical for PML localization and As_2O_3 responsiveness in vitro. Our observations suggest that acquired genetic mutations in the *PML-RARA* transcript may be a critical molecular mechanism of resistance to As_2O_3 therapy.

Methods

Patients

From January 2000 to December 2008 at Nagoya University Hospital, Japan, 15 patients with APL who showed relapse or disease progression

Submitted January 6, 2011; accepted May 9, 2011. Prepublished online as *Blood* First Edition paper, May 25, 2011; DOI 10.1182/blood-2011-01-329433.

The publication costs of this article were defrayed in part by page charge payment. Therefore, and solely to indicate this fact, this article is hereby marked "advertisement" in accordance with 18 USC section 1734.

An Inside *Blood* analysis of this article appears at the front of this issue.

Table 1. APL patients treated with As_2O_3 at Nagoya University Hospital

No.	Age, y	Sex	Diagnosis	Treatments prior to As_2O_3	Disease status at As_2O_3	Treatments after As_2O_3	Outcome	Survival after As_2O_3	As_2O_3 resistance
1	61	M	M3v	A+CT	Rel1	(−)	D	6 y, 1 mo	+
2	35	M	M3	A+CT	Rel1	sib-PBSCT	A	3 y, 8 mo	−
3	30	M	M3	A+CT	Rel2	auto-PBSCT	A	6 y, 9 mo	−
4	41	M	M3	A+CT	Rel1	auto-PBSCT	A	5 y, 8 mo	−
5	62	M	M3	A+CT, HD-Ara-C	Rel3	CBT	D	10 mo	−
6	42	F	M3	A+CT, aPBSCT	Rel2	CBT	D	4 mo	+
7	46	F	M3	A+CT	2nd CR	auto-PBSCT	A	6 y, 7 mo	−
8	54	F	M3	A+CT	Rel2	auto-PBSCT	A	5 y, 9 mo	−
9	19	M	M3	A+CT	Rel1	UR-BMT	A	6 y, 1 mo	−
10	42	M	M3	A+CT, UR-BMT	Rel3	DLI	A	6 y	−
11	61	M	M3v	A+CT	Rel1	(−)	D	4 mo	−
12	48	M	M3	A+CT, HD-Ara-C	Rel2	auto-PBSCT	A	4 y, 9 mo	−
13	39	M	M3v	A+CT, UR-BMT	Rel3	CBT	D	5 mo	−
14	20	M	M3	A+CT	Rel1	auto-PBSCT	A	4 y, 9 mo	−
15	36	M	M3	A+CT	Rel1	auto-PBSCT	A	4 y, 2 mo	−

Fifteen patients were treated with As_2O_3 at Nagoya University Hospital during the period of January 2000–December 2008. Outcomes were confirmed on December 1, 2009. Patients 5, 6, and 13 received cord blood transplantation after As_2O_3. Patients 5 and 13 died of complications of transplantation without any relapse sign. Patient 6 died of relapse just after transplantation. Patient 11 died of brain bleeding due to APL relapse with disseminated intravascular coagulation.

Rel1 through 3 indicates the first to third relapse; A+CT, ATRA with combination chemotherapy; PBSCT, peripheral blood stem cell transplantation; CBT, cord blood transplantation; BMT, bone marrow transplantation; D, dead; and A, alive.

after treatment with chemotherapy with ATRA were treated with As_2O_3 (Table 1). The diagnosis of APL and its relapse were confirmed by bone marrow morphology according to the FAB classification, chromosomal abnormality t(15;17) in peripheral blood and/or bone marrow cells, positive RT-PCR assay for *PML-RARA* transcripts, and/or FISH analysis of *PML* and *RARA*. As_2O_3 was diluted in 500 mL of 5% dextrose and administered intravenously over 2 hours at a dose of 0.15 mg/kg daily for a cumulative maximum of 60 days.

Patient 1 (Table 1 and Figure 1A) was diagnosed with APL (the microgranular variant M3v) in October 1998 (Figure 1A), and complete remission (CR) was obtained after combination chemotherapy with ATRA (45 mg/m^2/d). However, relapse with insufficient response to ATRA was observed (Figure 1A) after the end of consolidation therapy in August 1999. As_2O_3 (0.15 mg/kg/d) was started as a salvage chemotherapy, and a molecular response was obtained. The effectiveness of As_2O_3 gradually decreased during the patient's 7-year clinical course. Am80 (6 mg/m^2/d) was started in July 2005 in addition to As_2O_3 therapy. However, the effectiveness was poor, and Am80 was discontinued in October 2005. Thereafter, only As_2O_3 was used. At the terminal stage of his clinical course (Figure 1A), As_2O_3 was administered under the condition that $> 90\%$ of his peripheral blood cells were considered APL blast cells, but no response to the elevated blast count was observed. We diagnosed this condition as secondary As_2O_3 resistance. The patient died of disease progression in January 2006. During his 7-year clinical course, clinical samples from his bone marrow and/or peripheral blood were obtained repeatedly (Figure 1A).

Patient 6 was diagnosed with APL in January 2000, and CR was obtained after combination chemotherapy with ATRA. Relapse was observed in February 2002. After obtaining a second CR with combination chemotherapy, autologous peripheral blood stem cell transplantation was performed in October 2002. An early relapse was observed after transplantation in February 2003, and then As_2O_3 (0.15 mg/kg/d) was started. Partial cytoreduction was confirmed, but CR was not obtained. We diagnosed this condition as primary refractory disease to As_2O_3. As_2O_3 was used for 42 days and then discontinued. Cord blood transplantation was performed during non-CR, but the patient died of relapsed disease in July 2003. Genomic DNA was obtained from leukemia cells harvested 27 days after starting As_2O_3 therapy. Although the patient's bone marrow showed hypocellularity at this time, 97.1% of her marrow cells were positive for the *PML-RARA* fusion gene with FISH analysis.

Cell preparation from patients

After obtaining informed consent from each patient in accordance with the Declaration of Helsinki, the patients' primary cells were obtained from their peripheral blood and/or bone marrow. All experiments were conducted with institutional review board approval from the Nagoya University School of Medicine. Mononuclear cells were separated with Ficoll Paque (GE Healthcare) and preserved with CP-1 (Kyokuto Pharmaceutical Industrial) in liquid nitrogen until further analysis.

RNA extraction and RT-PCR

Total RNA was isolated from each sample using TRIzol (Invitrogen). cDNA was synthesized from 5 μg of total RNA using Superscript II reverse transcriptase (Invitrogen) as described previously.[26,27] PCR was performed using LA-Taq polymerase (Takara) under the following conditions: one cycle of 95°C for 4 minutes, followed by 40 cycles of 95°C for 30 seconds, 55°C for 30 seconds, and 72°C for 60 seconds. PCR primers for amplification of the coding sequences of *PML-RARA* are as follows: forward PR-U619: 5′-TGT TCC AAG CCG CTG T-3′, reverse PR-L2189: 5′-CAT CTT CAG CGT GAT CA-3′. Amplified PCR fragments were purified with a Wizard PCR prep DNA purification kit (Promega) and cloned into the pCR2.1-TOPO cloning vector (Invitrogen). At least 20 clones were sequenced with an ABI 310 automated DNA sequencer (Applied Biosystems). Genetic mutations were confirmed using MacVector Version 10.5.1 software.

Expression vectors

The coding sequence of *PML-RARA* was amplified with PCR, and the Flag sequence was added with the forward primer as described previously.[26,28] The PCR fragment was cloned into the pcDNA4-His-Max-TOPO mammalian expression vector (Invitrogen) to generate the following expression vectors: pcDNA4-XF-PR-WT for Xpress-tagged wild-type PML-RARA, pcDNA4-XF-PR-B/L-mut for Xpress-tagged PML-RARA with mutations resulting in A216V and G391E substitutions, pcDNA4-XF-PR-B2-mut for PML-RARA with the A216V substitution, and pcDNA4-XF-PR-L-B2-mut2 for the long-form PML-RARA with the L218P substitution. To express the long form of the wild-type PML-RARA protein, pcDNA4-XF-PR-L was used as described previously.[29] Expression vectors pcDNA-F-Ubc9, pcDNA-F-SUMO, and pcDNA-HA-PML for Flag-tagged Ubc9 and SUMO1, and HA-tagged PML, respectively, have also been described previously.[30]

Cell culture

Cells of the human cervical cancer cell line HeLa were cultured in DMEM containing 10% FCS. U937 cells, a human monocytic leukemia cell line, were cultured in RPMI containing 10% FCS.

Protein extraction and antibodies for immunoblotting

HeLa cells (1.0×10^5/well) were cultured in a 12-well plate for 12 hours before transfection. Transfection of the expression vectors was carried out using Effectene (Invitrogen) according to the manufacturer's instructions. The cells were washed with DMEM 24 hours after transfection, and then incubated for 8 hours with or without 10μM As_2O_3 (Sigma-Aldrich) until protein extraction. Whole-cell protein samples for immunoblotting were obtained using 250 μL of Laemmli sample buffer (200mM Tris-HCl, pH 6.8, 4% SDS, 20% glycerol, 10% 2-mercaptoethanol, and 0.004% bromophenol blue). After boiling for 5 minutes, samples were subjected to SDS-PAGE.

U937 cells were cultured in a 12-well plate for 12 hours before transfection. Transfection of the expression vectors pcDNA4-XF-PR-WT and pcDNA4-XF-PR-B/L-mut was carried out using Nucleofector Kit C (Lonza) according to the manufacturer's instructions. After 12 hours, immunofluorescent analysis was performed.

To separate PML-RARA protein into soluble and/or insoluble fractions, cells were lysed in 200 μL of RIPA lysis buffer (50mM Tris-HCl, pH 7.5, 150mM NaCl, 1% NP-40, 0.5% sodium deoxycholate, 0.1% SDS, 0.2mM PMSF, and a complete mini protease inhibitor tablet [Roche]). After centrifugation at 10 000*g* for 10 minutes, the supernatants were placed into new tubes, and 200 μL of 2× SDS sample buffer was added (soluble fraction). PBS (20 μL) and 200 μL of 2× SDS sample buffer were added to the pellets (insoluble fraction). After boiling for 5 minutes, samples were analyzed by SDS-PAGE followed by immunoblotting. Antibodies used in this assay are as follows: rabbit anti-hemagglutinin (anti-HA; Sigma-Aldrich), mouse anti-Xpress tag (Invitrogen), and mouse anti–FLAG-M2 (Sigma-Aldrich).

Immunofluorescence microscopy

HeLa cells expressing Flag- and Xpress-tagged PML-RARA and its mutated proteins were cultured on Chamber Slides (Lab-Tek) with or without 10μM As_2O_3. U937 cells expressing Flag- and Xpress-tagged PML-RARA and its mutated proteins and the primary leukemia cells were placed on slide glasses using Cytospin (Shandon Southern Products), air dried, and fixed in acetone/methanol for 10 minutes at −20°C. Cells were then blocked with 1% BSA (Sigma-Aldrich) in PBS for 1 hour, incubated with primary antibodies for 3 hours, and incubated with Alexa Fluor 488 (green)- or 568 (red)–conjugated secondary antibodies for 1 hour at room temperature. Antibodies used in this assay are as follows: rabbit anti–human PML (Santa Cruz Biotechnology), mouse anti–FLAG-M2 (Sigma-Aldrich), rabbit Alexa Fluor 488 (Invitrogen), and mouse Alexa Fluor 568 (Invitrogen). The slides were examined with an Axioskop 2 fluorescence microscope (Carl Zeiss), photos were taken and analyzed with AxioVision FRET Release 4.5, and images were processed with Adobe Photoshop CS3 software.

Results

Two of 15 patients showed clinical As_2O_3 resistance

From January 2000 to December 2008 in Nagoya University Hospital, 15 relapsed patients with APL, including 3 with M3v,[31] were treated with As_2O_3 (Table 1). As a first-line treatment, combination chemotherapies with ATRA were administered to all patients. Thirteen patients received autologous or allogeneic stem cell transplantation after treatment with As_2O_3, and long-term remission (range, 44-81 months) was confirmed in 10 patients. One patient (patient 1; see also "Patients") showed resistance to As_2O_3 after repeated therapy. Another patient (patient 6; see also "Patients") showed resistance to the first course of As_2O_3 therapy. Disease progression (elevation of the blast count in the peripheral blood) was observed in patient 1 after long-term treatment with As_2O_3, and primary refractory disease that was resistant to As_2O_3 was confirmed in patient 6. Both patients died after disease progression.

Acquired missense mutations in PML-RARA transcripts observed in the 2 patients with As_2O_3 resistance

To determine the molecular mechanisms of the resistance to As_2O_3, we first focused on patient 1 who had a long clinical course and whose clinical samples had been preserved several times at each disease stage.

Total RNA was extracted from each sample, and RT-PCR for *PML-RARA* transcripts was performed. DNA sequencing analysis using the sample obtained from the terminal stage was performed first (Figure 1A sample 5). The *PML-RARA* transcript was a short-form type (bcr3[32]) that lacked the nuclear localizing signal (NLS) in PML. Missense mutations resulting in the A216V substitution in the PML-B2 domain and the G391E substitution in the RARA ligand-binding domain (LBD; Figure 1B) were detected. The predicted mutated PML-RARA protein resulting from these mutations is shown in Figure 2A.

We then determined the sequence of *PML-RARA* in patient #6, who showed primary refractory disease to As_2O_3. Only a limited clinical sample obtained at 27 days after starting the As_2O_3 treatment was available for genomic analysis. A missense mutation resulting in an L218P substitution in the PML-B2 domain was confirmed in 2 of 20 clones with PCR cloning using genomic DNA PCR (Figure 1C). The mutations in the PML-B2 domain are indicated as B2-mut and B2-mut2 in Figure 1D. The predicted mutated PML-RARA protein designated as PR-L-B2-mut2 is also shown in Figure 2A. The location of these mutations is very close to the As_2O_3-binding cysteine-cysteine (CC) motif reported by Jeanne et al.[25]

Clonal expansion of PR-B/L-mut at the terminal stage of APL disease progression

To confirm the clonal expansion of the genetic mutations in *PML-RARA*, we performed sequencing analysis using the RT-PCR fragments of *PML-RARA* transcripts from the serial clinical samples obtained from patient 1 (samples 1-5 in Figure 1A). PCR fragments were cloned into the vector, and at least 20 clones were picked for sequencing analysis. Genetic mutations resulting in PR-B2-mut, PR-LBD-mut, and PR-B/L-mut (Figure 2A) were confirmed in samples 4 and 5 obtained at this patient's terminal stage when As_2O_3 resistance and the expansion of the blast count were clinically observed (Figure 2B). These clones were not confirmed in samples 1-3, and the partial response to As_2O_3 treatment was confirmed at the periods 2-3. The samples 2 and 3 had blasts showing FISH-positive *PML-RARA* clones (33.9% and 74.0%, respectively). This result strongly suggests that these mutations were closely related to disease progression during As_2O_3 treatment.

Lack of multimerization of PR-B/L-mut with and without As_2O_3

Posttranslational modification of PML, including SUMOylation, is reported to be critical for the responsiveness to As_2O_3.[24,25,33] To confirm the functional difference between PR-WT and its mutant, we performed an in vitro SUMOylation assay in HeLa cells. HA-tagged PML, Xpress-tagged PR-WT, PR-B/L-mut, and SUMO1/Ubc9 were expressed in HeLa cells with or without 10μM As_2O_3 (Figure 3A-B). PML, PR-WT, and PR-B/L-mut were detected with immunoblotting. SUMO1/Ubc9 is coexpressed with PML, and therefore, SUMOylated PML bands were observed (indicated with black triangles in Figure 3A lane 2). The intensity of the mobility-shifted bands was increased with As_2O_3 treatment (Figure 3A lane 3). When using PR-WT, multimerized/SUMOylated

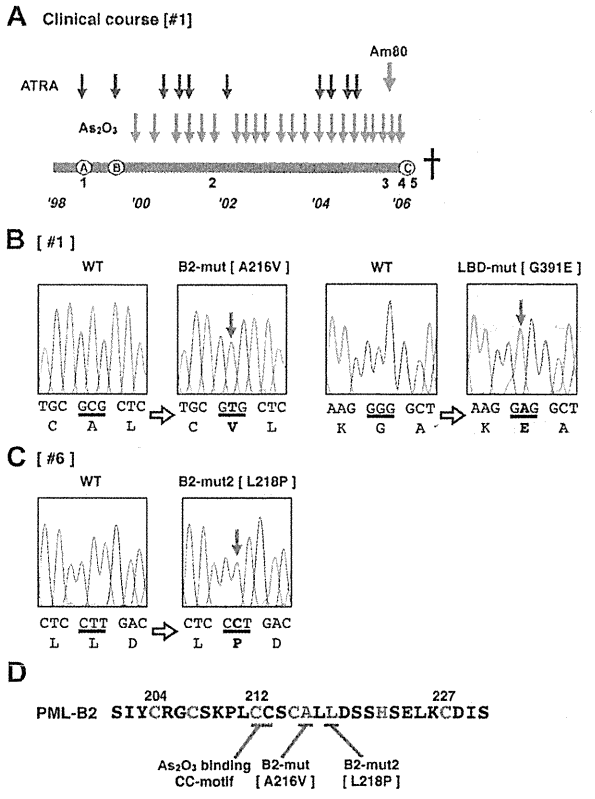

Figure 1. Additional genetic mutations in *PML-RARA* in patients showing an As_2O_3 refractory/resistant phenotype. (A) Clinical course of patient 1, who showed As_2O_3 resistance in the terminal stage of disease progression. The total clinical duration of the patient was almost 7 years. Detailed information is described in "Methods." Black and gray arrows indicate the course of chemotherapies with ATRA, As_2O_3, and Am80. The letters A-C enclosed in circles indicate clinically important time points: A indicates diagnosis with APL, B indicates relapse with inadequate response to ATRA, and C indicates confirmation of clinical As_2O_3 resistance. This patient died of disease progression. Leukemia cells from the bone marrow and peripheral blood were obtained at time periods 1-5. Genetic mutations in *PML-RARA* were confirmed in patients 1 (B) and 6 (C). Missense point mutations in the PML B2 domain and RARA LBD domain were confirmed in the leukemia cells from time point 5. DNA sequences and the genetic code are indicated in capital letters. Bold letters indicate mutations. (D) The zinc finger motif of the PML-B2 domain. Amino acid substitutions in patients 1 and 6 are depicted. The CC motif critical for As_2O_3 binding[25] is also indicated. The "C" and "H" in red are the cysteine and histidine, respectively, which are important for zinc finger formation.

PR-WT bands were confirmed with and without As_2O_3 (Figure 3B lanes 4-6 black triangles). However, when using PR-B/L-mut, oligomerized/SUMOylated PML-RARA protein was not observed with SUMO1/Ubc9 with or without As_2O_3 (Figure 3B lanes 8 and 9). When PR-B2-mut was used in the same assay system, nearly the same result was obtained (Figure 3B lanes 11 and 12). These results indicate that the genetic mutation leading to amino acid alteration of the PML-B2 domain is critical for the appropriate posttranslational modification of the PML-RARA protein, including SUMOylation and oligomerization.

Distinct cellular localization of PR-WT and PR-B/L-mut in soluble/insoluble fractions

Recently, it has been reported that As_2O_3 promotes PML-RARA multimerization via disulfide-mediated covalent binding, leading to formation of PML nuclear bodies; these multimers are subsequently SUMOylated.[25] To confirm the cellular localization (soluble/insoluble fractions, see also "Methods") of PML, PR-WT, and PR-B/L-mut with or without As_2O_3, we performed immunoblotting using HeLa cells that were transiently overexpressing each protein. Cells were lysed using RIPA buffer, as described previously,[14,24] and the whole-cell lysate was separated into 2 fractions, soluble (supernatant) and insoluble (pellet). In the absence of As_2O_3, PML was localized in both the soluble and insoluble fractions (Figure 4A lanes 1 and 3). With As_2O_3, PML was detected mostly in the insoluble fraction (Figure 4A lanes 2 and 4). Nearly the same results were obtained with PR-WT (short form of PML-RARA, Figure 4B lanes 5, 6, 11, and 12) and PR-long (long form of PML-RARA, Figure 4B lanes 9, 10, 15, and 16). Conversely, PR-B/L-mut was localized in both the soluble and insoluble fractions with and without As_2O_3, and protein modification including multimerization was not observed with this assay system (Figure 4B lanes 7, 8, 13, and 14). Protein expression levels were quantitated with BioMax software, and the relative intensity is depicted in Figure 4C. These findings indicate that As_2O_3 did not affect PR-B/L-mut compared with PML and PR-WT in this assay system, and this phenomenon was closely related to insufficient SUMOylation (Figure 3).

Distinct cellular localization of PR-WT and PR-B/L-mut with or without As_2O_3 in HeLa and U937 cells

We then performed immunofluorescent (IF) staining to examine the cellular localization pattern of wild-type PML, PR-WT, and PR-B/L-mut in HeLa cells (Figure 5). Wild-type PML was overexpressed in HeLa cells, which were incubated with or without As_2O_3. PML localization was confirmed by IF staining using an anti-PML antibody. PML was localized in PML nuclear bodies showing a speckled pattern without As_2O_3 (Figure 5Ai,iii). In the presence of As_2O_3, the localization pattern was clearly altered to a macrogranular pattern (Figure 5Aiv,vi).

Similar analyses using PR-WT- and PR-B/L-mut–expressing HeLa cells were also performed (Figure 5B-C). Anti-PML antibody was used to detect endogenous PML, overexpressed PR-WT, and PR-B/L-mut, and anti-Flag antibody was used to detect PR-WT and PR-B/L-mut. In the absence of As_2O_3, PR-WT, a PML-RARA short form without an NLS, was detected around the nucleus as a microgranular pattern (Figure 5Bi,ii,iv), and as a macrogranular pattern in the presence of As_2O_3 (Figure 5Bv,vi, and viii). Surprisingly, PR-B/L-mut was localized differently in the cytoplasm as a diffuse pattern without As_2O_3 (Figure 5C,i,ii,iv), and the localization of PR-B/L-mut was not altered in the presence of As_2O_3 (Figure 5Cv,vi,viii). With As_2O_3 treatment, endogenous PML was confirmed in the nucleus with the macrogranular pattern (Figure 5Cv,viii). Transfected PR-B/L-mut (red fluorescence) could not be confirmed in the nucleus (Figure 5Cvi). The localization of PR-B2-mut showed almost the same pattern as PR-B/L-mut (data not shown). These data strongly suggest that the point mutation in the PML-B2 domain disrupts or inhibits PML body formation and the responsiveness to As_2O_3 treatment.

Nearly identical analyses using U937 cells were performed to confirm the significance in hematopoietic cells. As indicated in Figure 5D, PR-WT was observed in the cytoplasm with the microgranular pattern (Figure 5Di,ii,iv), and PR-B/L-mut showed a diffuse pattern, as observed in HeLa cells (Figure 5Dv,vi,viii).

Distinct cellular localization of PR-L and PR-L-B2-mut2 with or without As_2O_3 in HeLa cells

We also performed a similar analysis using PR-L and PR-L-B2-mut2 to show the molecular significance of the L218P mutation

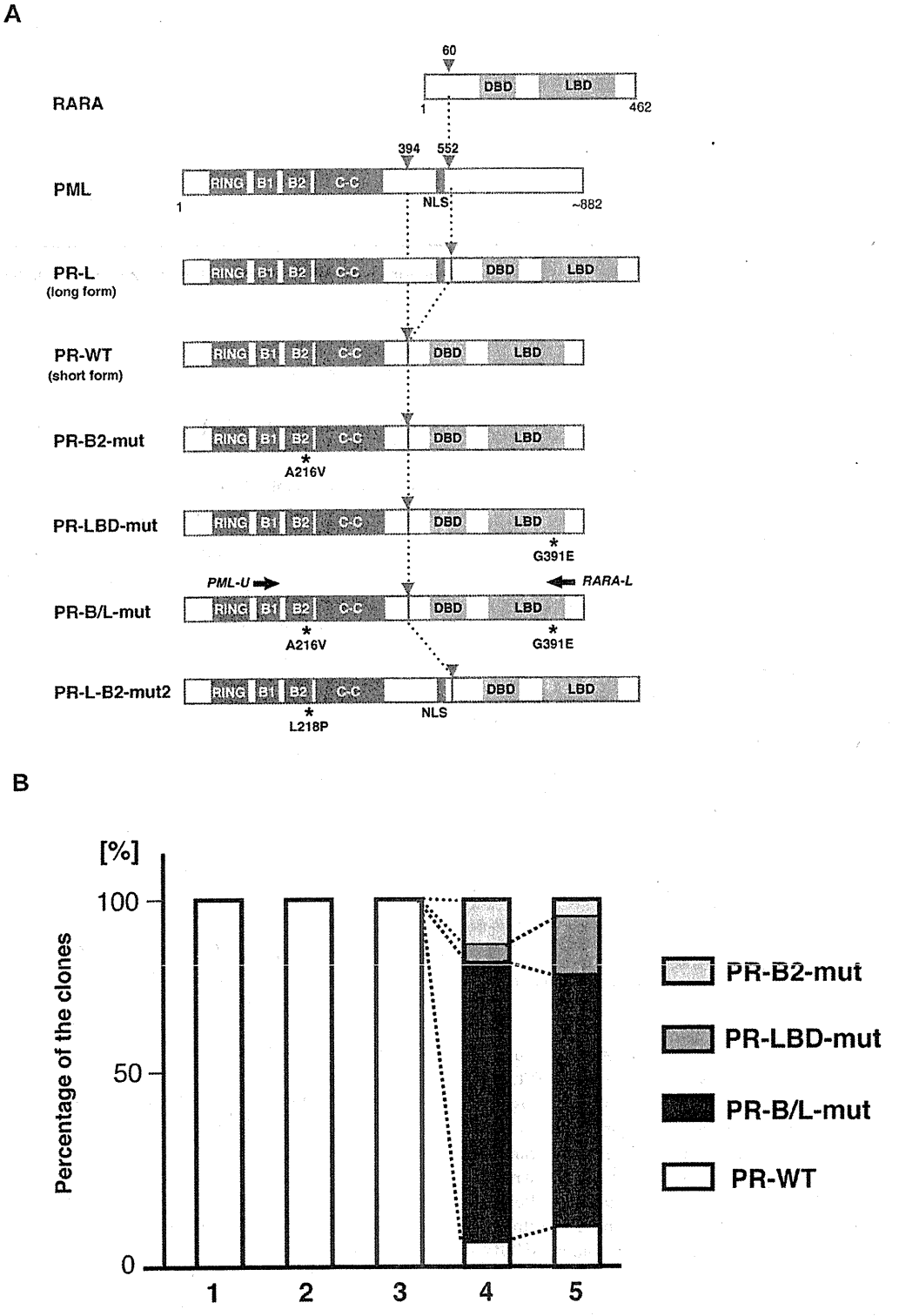

Figure 2. Clonal expansion of PML-B2 and RARA-LBD mutations during disease progression. (A) Schematic representation of PML, RARA, and its fusion proteins with or without mutations. Functional domains are indicated. Gray arrowheads indicate the break points of the fusion proteins. Black asterisks depict amino acid substitutions resulting from genetic mutations. Black arrows indicate the positions of the PCR primers for amplifying *PML-RARA* fusion transcripts. RING indicates the RING finger; B1 and B2, B-box motifs; C-C, coiled-coil; and DBD, DNA-binding domain. (B) Clonal expansion of *PML-RARA* mutants. Using the clinical samples obtained at time points 1-5 in Figure 1A, RT-PCR using PCR primers (PML-U and RARA-L in Figure 1A) followed by cloning was performed. At least 20 clones were sequenced for each sample. The percentages of the clones are depicted in the bar graph.

in the B2 domain confirmed in patient 6 (Figure 6). PR-L, a PML-RARA long form with an NLS, was detected in the nucleus as a microgranular pattern without As_2O_3 (Figure 6Ai,ii,iv) and as a macrogranular pattern with As_2O_3 (Figure 6Av,vi,viii). In contrast, PR-L-B2-mut2 was localized in the nucleus as a diffuse pattern without As_2O_3 (Figure 6Bi,ii,iv). The localization was not altered in

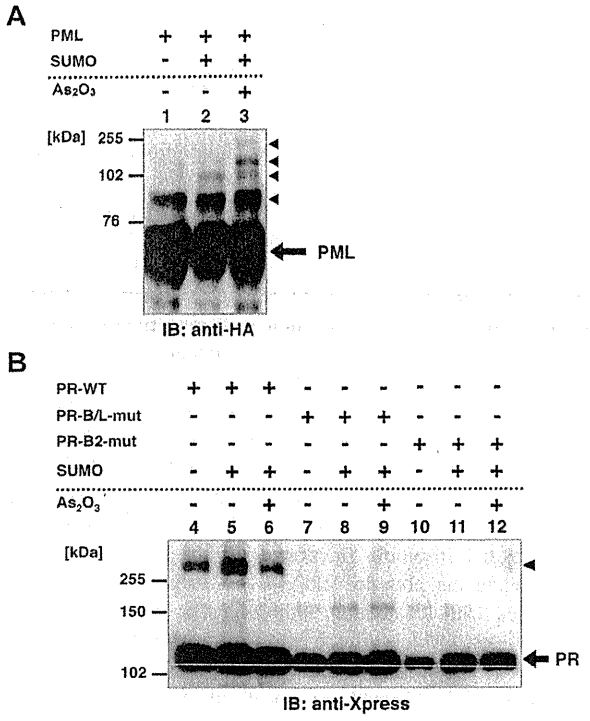

Figure 3. Posttranslational modification of PML, PR-WT, PR-B/L-mut, and PR-B2-mut induced by SUMO1/Ubc9. (A) HA-tagged PML and SUMO1/Ubc9 (SUMO) expression vectors were transfected into HeLa cells as indicated and incubated with or without As_2O_3 (10μM) for 8 hours. Immunoblot analysis using an anti-HA antibody was carried out. Black arrowheads indicate SUMO-modified PML. (B) Xpress-tagged PR-WT, PR-B/L-mut, or PR-B2-mut was overexpressed in HeLa cells with or without SUMO1/Ubc9 and incubated with or without As_2O_3 (10μM) for 8 hours. Black arrowhead indicates SUMO-modified/dimerized PR-WT (lanes 4-6). Note that the modified bands of PR-B/L-mut and PR-B2-mut were barely detected (lanes 7-12).

the presence of As_2O_3 (Figure 6Bv,vi,viii). These data strongly suggest that the L218P mutation in the PML-B2 domain contributes to the aberrant PML body formation and disrupts responsiveness to As_2O_3 treatment.

Cellular localization of endogenous PR-B/L-mut without As_2O_3 in primary cells from a patient

To show the localization of PR-WT and PR-B/L-mut protein in primary leukemia cells, IF staining using an anti-PML antibody was performed (Figure 7). Primary leukemia cells from patient 1 obtained at diagnosis and at the terminal stage were used to detect PR-WT and PR-B/L-mut, respectively. Nearly the same localization pattern as seen in Figure 5 was confirmed in this assay. The PML bodies were observed as a granular pattern at diagnosis (PR-WT), but the pattern was significantly altered to become diffuse at the terminal stage (PR-B/L-mut). These data strongly suggest that PR-B/L-mut protein was expressed and functional in primary leukemia cells, and may contribute to different responsiveness to As_2O_3 treatment.

Discussion

In the present study, we have shown acquired missense mutations in *PML-RARA* that are closely related to resistance to As_2O_3 treatment. In 2 patients, we detected A216V and L218P substitutions in the B2 domain of PML. The B2 domain is part of the RBCC motif, which is thought to be critical for PML homo/

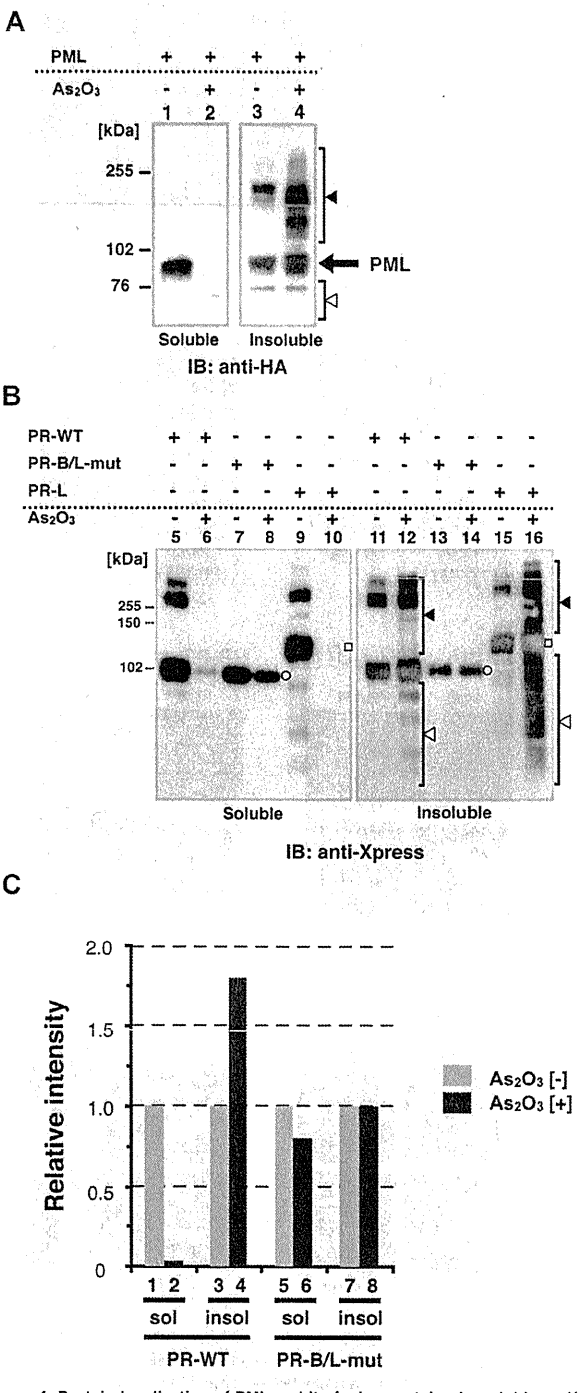

Figure 4. Protein localization of PML and its fusion proteins in soluble and/or insoluble fractions with or without As_2O_3. (A) HA-PML was overexpressed in HeLa cells with or without As_2O_3 (10μM for 2 hours), and the whole-cell lysate (soluble) and pellets (insoluble fraction) were obtained for immunoblotting. Black and white arrowheads indicate modified/oligomerized and degraded PML, respectively. (B) The same assay described in panel A was performed using PR-WT, PR-B/L-mut, and the long form of PML-RARA (PR-long). White circles indicate PR-WT or PR-B/L-mut and white squares indicate PR-long protein. Black and white arrowheads indicate modified/oligomerized and degraded fusion proteins, respectively. Note that neither protein transportation from the soluble to insoluble fraction (lanes 7 vs 8 and 13 vs 14) nor modified/oligomerized or degraded proteins after treatment with As_2O_3 (lanes 8 and 14) were observed with PR-B/L-mut. (C) Protein expression levels in panel B were measured using BioMax 1D software, and the relative intensity is depicted as a bar graph.

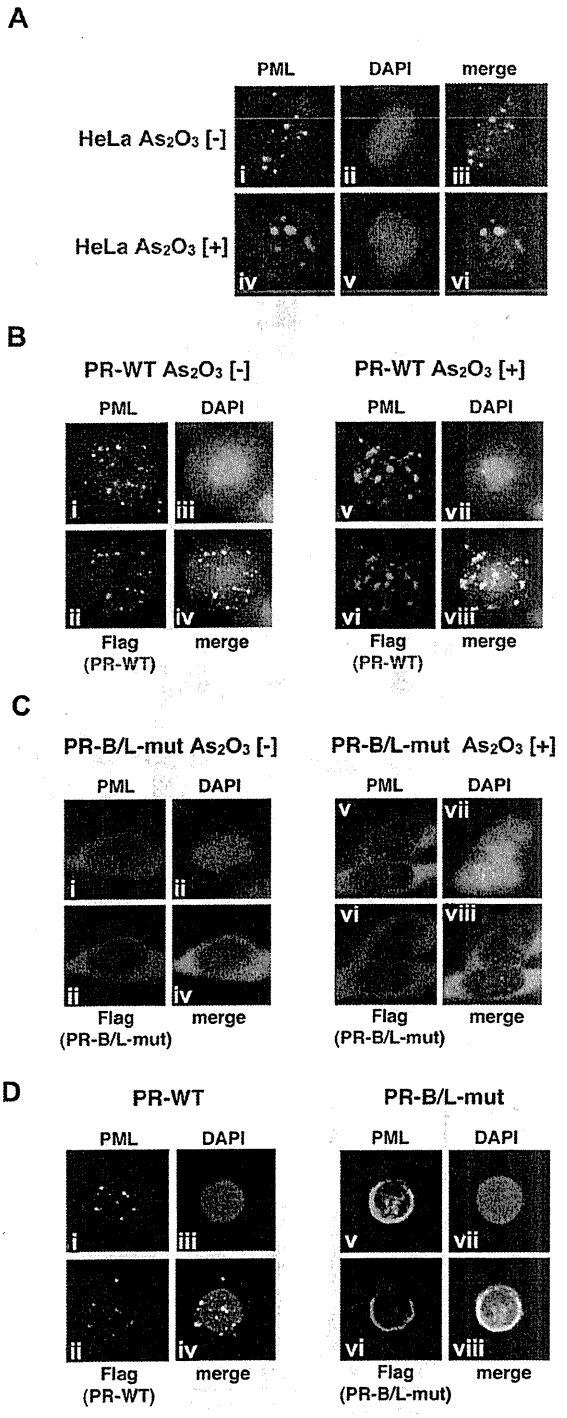

Figure 5. Analyses of the protein localization of PML, PR-WT, and PR-B/L-mut using IF staining. (A) HeLa cells were incubated with or without As_2O_3 (10μM) for 8 hours, and endogenous PML was detected with an anti-PML antibody. PML nuclear bodies were detected in green. The nuclei were stained with 4,6 diamidino-2-phenylindole (DAPI; blue). Note that the microgranular pattern of NBs without As_2O_3 (i and iii) was altered to become a macrogranular pattern with As_2O_3 (iv and vi). (B) Flag-tagged PR-WT was used for the same assay as described in panel A. Anti-FLAG and anti-PML antibodies were used to detect PR-WT and endogenous PML, respectively. PML bodies were confirmed in the cytoplasm with a microgranular pattern without As_2O_3 (i,ii, and iv) and a macrogranular pattern with As_2O_3 (v,vi, and viii). (C) When using Flag-tagged PR-B/L-mut, localization showed a diffuse pattern mostly in the cytoplasm with and without As_2O_3. (D) Flag-tagged PR-WT or PR-B/L-mut was overexpressed in U937 cells without As_2O_3, and the same IF staining was performed. Note that PR-B/L-mut localization was confirmed in the cytoplasm as a diffuse pattern. Magnification is 800×.

heterodimerization, oligomerization, and As_2O_3 binding.[23-25,34] Recent studies have indicated that As_2O_3 binds directly to cysteine residues in zinc fingers in the RBCC domain, especially C77/80 and C88/91 in the RING domain[24] and C212 and C213 in the B2 domain.[25] Binding of As_2O_3 in the RBCC domain appears to be critical for the effect of As_2O_3 on PML-RARA.[24,25] Interestingly, the mutations described herein were located just adjacent to the CC motif (C212/213) in the B2 domain, which is thought to be critical for As_2O_3 binding (Figure 1D). These findings suggest that substitutions at A216 and L218 may affect proper As_2O_3 binding, resulting in aberrant responsiveness to As_2O_3 through aberrant subcellular localization, insufficient SUMOylation, and/or multimerization.

The in vitro SUMOylation assay indicated that PR-B/L-mut and PR-B2-mut mostly lack SUMO1-Ubc9–induced SUMOylation and dimerization/multimerization (Figure 3B), and this was not changed in the presence of As_2O_3. It has been suggested that degradation of the PML-RARA protein with As_2O_3, followed by SUMOylation and oligomerization,[24,25] may also be inhibited by mutations in the B2 domain. Furthermore, PR-B/L-mut was localized in both the soluble and insoluble fractions, and the localization was not changed in the presence of As_2O_3. Nearly the same result was obtained with IF staining, indicating that PR-B/L-mut and PR-B2-mut were localized in the cytoplasm with a diffuse pattern that was not altered in the presence of As_2O_3 (Figure 5C). Furthermore, PR-L-B2-mut2 was localized in the nucleus as a diffuse pattern with or without As_2O_3 (Figure 6B). These results strongly suggest that amino acid substitution in the B2 domain is

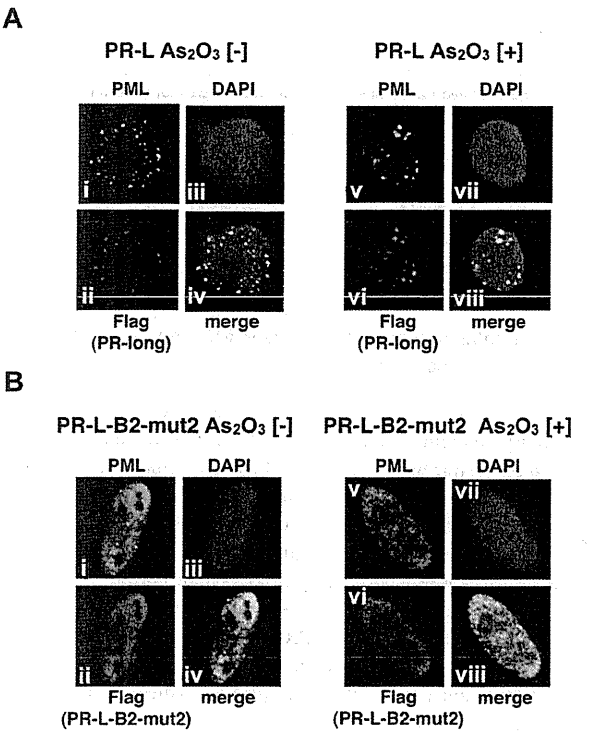

Figure 6. Analyses of the protein localization of PR-L and PR-L-B2-mut2 using IF staining. (A) Flag-tagged PR-L was overexpressed in HeLa cells with or without As_2O_3. Anti-FLAG and PML antibodies were used to detect PR-L and endogenous PML, respectively. PML bodies were confirmed in the nucleus with a microgranular pattern without As_2O_3 (i,ii, and iv) and a macrogranular pattern with As_2O_3 (v,vi, and viii). (B) A similar assay was performed using PR-L-B2-mut2. Note that the localization of PR-L-B2-mut2 was confirmed in the nucleus as a diffuse pattern with or without As_2O_3.

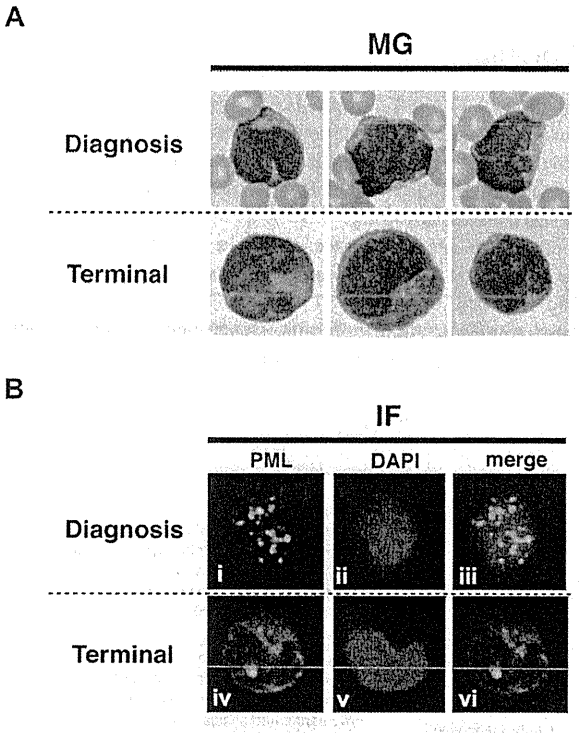

Figure 7. Protein localization of PML and its fusion proteins in primary leukemia cells from patient #1. May-Giemsa (MG) staining (A) and IF staining (B) are shown. The primary leukemia cells from patient 1 were obtained at diagnosis and at the terminal stage (shown as 1 and 5, respectively, in Figure 1A) and were used in this assay. PML nuclear bodies can be observed in the cells at diagnosis (i and iii), but at the terminal stage, PML and its fusion proteins were observed in the cytoplasm showing a diffuse pattern (iv and vi).

critical for the aberrant responsiveness in vitro, and the mutations may be critical for the resistance to As_2O_3 therapy in vivo.

In patient 6, only 2 of 20 clones (10%) contained a genetic mutation resulting in an L218P substitution in the B2 domain of the PML region. The genetic mutation was theoretically present in 20% of bone marrow cells, and the remaining 77% of leukemia cells (*PML-RARA*–positive cells [97.1%] in FISH analysis included *PML-RARA*–mutated cells [20%]) harbored wild-type PML-RARA according to the FISH analysis. Careful evaluation of whether the mutation contributes to clinical resistance to As_2O_3 therapy should be performed. Because clinically refractory disease against As_2O_3 was confirmed after the bone marrow aspiration, clonal expansion of PML-RARA with the L218P substitution may have been related to the insufficient responsiveness to As_2O_3 therapy. Another question is when the mutated clone appeared in this patient. One possibility is that the mutated clone was already present at the early stage of the disease. Genetic analysis using DNA obtained at the disease onset may be useful for clarifying this. Unfortunately, DNA obtained at the disease onset and the terminal stage of this patient was not available, and clarifying these issues is not currently possible. Further examination of additional patients and genetic analyses of samples obtained at several time points during the disease progression are required.

Interestingly, PR-B/L-mut was localized in the cytoplasm (Figures 5C and 6B), not in the nucleus. As reported previously, an NLS on the PML C-terminus is critical for transport into the nucleus.[35,36] The absence of an NLS motif in the short form of PML-RARA (bcr3)[32,37,38] may explain the cytoplasmic localization of PR-WT and PR-B/L-mut in our study. Furthermore, PR-B/L-mut and -B2-mut showed a diffuse pattern (Figures 5C-D, 6B, and 7B). Borden et al[34] reported that substitution of conserved zinc finger domains in B1 and/or B2 disrupts PML nuclear body formation in vivo, and they also suggested that B1/B2 domains may be involved in the homo/hetero-oligomerization process via protein-protein interactions. Other studies have indicated that PML-RARA with mutations in B2 show a diffuse cytoplasmic pattern, perhaps because the mutated proteins cannot bind to nuclear body–forming proteins such as Daxx, Sp100, and SUMO-1, resulting in a failure to accumulate in the nuclear body.[24,25,39,40] Amino acid substitution near the zinc finger motif in the B2 domain may lead to conformational changes in the PML protein. Further analyses are needed.

PR-B/L-mut also contains a mutation in the LBD of RARA (G391E). Previous studies have indicated that the LBD mutation is closely related to ATRA resistance,[41-44] and patient 1 in this study also showed a clinically refractory response to ATRA in the late stage of his disease progression and resistance to Am80 in the terminal stage. The LBD mutation G391E was detected only in the terminal stage (Figure 2B lanes 4 and 5). Therefore, an APL variant phenotype with bcr3 of the PML-RARA protein may be related to a poor prognosis,[32,37,38] showing that insufficient ATRA effectiveness and the LBD mutation are related to a consistent phenotype of ATRA resistance.[45] PR-B/L-mut is localized mainly in the cytoplasm, and the effectiveness of ATRA may not be anticipated. The function of PR-WT and PR-B/L-mut as transcription factors to control activation and/or repression by recruiting coregulators, such as p300/CBP, SMRT/N-CoR-TBL1/R1, and histone deacetylases,[26,29,46,47] should be analyzed to confirm the responsiveness to ATRA. Conversely, the probability of the effects of the LBD mutation on As_2O_3 resistance may be relatively low based on our experiment, because the diffuse localization pattern in the cytoplasm of PR-B2-mut without an LBD mutation in the presence or absence of As_2O_3 showed nearly the same pattern as PR-B/L-mut (data not shown). Furthermore, a previous study indicated that ATRA-resistant NB4 clones with mutations in the PML-RARA LBD domain were fully sensitive to As_2O_3 treatment.[48]

Interestingly, leukemia cells from patient 1 contained minor clones of PR-B2-mut and PR-LBD-mut in addition to the major clone of PR-B/L-mut at the terminal stage (Figure 2B time points 4 and 5), which is difficult to explain. One possibility is that one allele of the wild-type *PML* and *RARA* genes originally had genetic mutations in the B2 and LBD domains, and PR-WT, PR-B2-mut, PR-LBD-mut, and PR-B/L-mut were generated at the early stage of disease progression. Another explanation is that the *PML-RARA* fusion gene with mutations in the B2 and LBD domains translocated again with wild-type *PML* or *RARA* genes during the disease progression. Further analyses are required using several strategies including allele-specific PCR, FISH, and/or single nucleotide polymorphism analysis.

Mutations in the B2 domain that result in insufficient responsiveness to As_2O_3 therapy were confirmed in 2 of 15 (13%) patients with APL treated with As_2O_3. Recently, As_2O_3 was introduced as a consolidation treatment, and the event-free survival at 3 years was significantly improved compared with conventional consolidation treatment with ATRA and daunorubicin (80% vs 63%).[12] However, almost 5% of patients with APL treated with As_2O_3 show As_2O_3 refractory disease.[49] Because it is possible that a PML B2 mutation may be partly related to the As_2O_3 refractory phenotype, repeated genetic analyses at several time points of the clinical course may be useful for predicting patients at high risk for a poor

response to As_2O_3 therapy. Further investigation is required to confirm the clinical significance.

Acknowledgments

The authors thank Nobuhiko Emi, Kazuhito Yamamoto, Yukiyasu Ozawa, Taku Kimura, Keiko Niimi, Hiroshi Sao, Kazunori Ohnishi, and Hidehiko Saito for caring for the patients with APL and Tomoka Wakamatsu, Eriko Ushida, Manami Kira, Mari Otsuka, and Yukie Konishi for valuable laboratory assistance.

This work was supported by grants-in-aid for scientific research from the Ministry of Education, Culture, Sports, Science and Technology, Japan, and from the Public Trust Haraguchi Memorial Cancer Research Fund, Japan.

Authorship

Contribution: E.G., A.T., and F.H. designed the experiments, performed the research, and the analyzed data; E.G. and A.T. wrote the manuscript; A.A. prepared the clinical samples and performed the research; and A.T., H.K., and T.N. interpreted the data and supervised the experiments.

Conflict-of-interest disclosure: H.K. is a consultant for Kyowa Hakko Kogyo Co Ltd. The remaining authors declare no competing financial interests.

Correspondence: Akihiro Tomita, Department of Hematology and Oncology, Nagoya University Graduate School of Medicine, Tsurumai-cho 65, Showa-ku, Nagoya 466-8550, Japan; e-mail: atomita@med.nagoya-u.ac.jp.

References

1. Kakizuka A, Miller WH Jr, Umesono K, et al. Chromosomal translocation t(15;17) in human acute promyelocytic leukemia fuses RAR alpha with a novel putative transcription factor, PML. *Cell.* 1991;66(4):663-674.
2. Huang ME, Ye YC, Chen SR, et al. Use of all-trans retinoic acid in the treatment of acute promyelocytic leukemia. *Blood.* 1988;72(2):567-572.
3. Ohno R, Yoshida H, Fukutani H, et al. Multi-institutional study of all-trans-retinoic acid as a differentiation therapy of refractory acute promyelocytic leukemia. Leukaemia Study Group of the Ministry of Health and Welfare. *Leukemia.* 1993;7(11):1722-1727.
4. Kanamaru A, Takemoto Y, Tanimoto M, et al. All-trans retinoic acid for the treatment of newly diagnosed acute promyelocytic leukemia. Japan Adult Leukemia Study Group. *Blood.* 1995;85(5):1202-1206.
5. Lo-Coco F, Avvisati G, Vignetti M, et al. Front-line treatment of acute promyelocytic leukemia with AIDA induction followed by risk-adapted consolidation for adults younger than 61 years: results of the AIDA-2000 trial of the GIMEMA Group. *Blood.* 2010;116(17):3171-3179.
6. Sanz MA, Montesinos P, Vellenga E, et al. Risk-adapted treatment of acute promyelocytic leukemia with all-trans retinoic acid and anthracycline monochemotherapy: long-term outcome of the LPA 99 multicenter study by the PETHEMA Group. *Blood.* 2008;112(8):3130-3134.
7. Asou N, Kishimoto Y, Kiyoi H, et al. A randomized study with or without intensified maintenance chemotherapy in patients with acute promyelocytic leukemia who have become negative for PML-RARalpha transcript after consolidation therapy: the Japan Adult Leukemia Study Group (JALSG) APL97 study. *Blood.* 2007;110(1):59-66.
8. Niu C, Yan H, Yu T, et al. Studies on treatment of acute promyelocytic leukemia with arsenic trioxide: remission induction, follow-up, and molecular monitoring in 11 newly diagnosed and 47 relapsed acute promyelocytic leukemia patients. *Blood.* 1999;94(10):3315-3324.
9. Wang ZY, Chen Z. Acute promyelocytic leukemia: from highly fatal to highly curable. *Blood.* 2008;111(5):2505-2515.
10. Shen ZX, Chen GQ, Ni JH, et al. Use of arsenic trioxide (As2O3) in the treatment of acute promyelocytic leukemia (APL): II. Clinical efficacy and pharmacokinetics in relapsed patients. *Blood.* 1997;89(9):3354-3360.
11. Soignet SL, Frankel SR, Douer D, et al. United States multicenter study of arsenic trioxide in relapsed acute promyelocytic leukemia. *J Clin Oncol.* 2001;19(18):3852-3860.
12. Powell BL, Moser B, Stock W, et al. Arsenic trioxide improves event-free and overall survival for adults with acute promyelocytic leukemia: North American Leukemia Intergroup Study C9710. *Blood.* 2010;116(19):3751-3757.
13. Emadi A, Gore SD. Arsenic trioxide - An old drug rediscovered. *Blood Rev.* 2010;24(4-5):191-199.
14. Zhu J, Koken MH, Quignon F, et al. Arsenic-induced PML targeting onto nuclear bodies: implications for the treatment of acute promyelocytic leukemia. *Proc Natl Acad Sci U S A.* 1997;94(8):3978-3983.
15. Müller S, Matunis MJ, Dejean A. Conjugation with the ubiquitin-related modifier SUMO-1 regulates the partitioning of PML within the nucleus. *EMBO J.* 1998;17(1):61-70.
16. Lallemand-Breitenbach V, Zhu J, Puvion F, et al. Role of promyelocytic leukemia (PML) sumolation in nuclear body formation, 11S proteasome recruitment, and As2O3-induced PML or PML/retinoic acid receptor alpha degradation. *J Exp Med.* 2001;193(12):1361-1371.
17. Tatham MH, Geoffroy MC, Shen L, et al. RNF4 is a poly-SUMO-specific E3 ubiquitin ligase required for arsenic-induced PML degradation. *Nat Cell Biol.* 2008;10(5):538-546.
18. Sun Y, Kim SH, Zhou DC, et al. Acute promyelocytic leukemia cell line AP-1060 established as a cytokine-dependent culture from a patient clinically resistant to all-trans retinoic acid and arsenic trioxide. *Leukemia.* 2004;18(7):1258-1269.
19. Dai J, Weinberg RS, Waxman S, Jing Y. Malignant cells can be sensitized to undergo growth inhibition and apoptosis by arsenic trioxide through modulation of the glutathione redox system. *Blood.* 1999;93(1):268-277.
20. Davison K, Cote S, Mader S, Miller WH. Glutathione depletion overcomes resistance to arsenic trioxide in arsenic-resistant cell lines. *Leukemia.* 2003;17(5):931-940.
21. Kitamura K, Minami Y, Yamamoto K, et al. Involvement of CD95-independent caspase 8 activation in arsenic trioxide-induced apoptosis. *Leukemia.* 2000;14(10):1743-1750.
22. Borden KL, Campbell Dwyer EJ, Salvato MS. An arenavirus RING (zinc-binding) protein binds the oncoprotein promyelocyte leukemia protein (PML) and relocates PML nuclear bodies to the cytoplasm. *J Virol.* 1998;72(1):758-766.
23. Saurin AJ, Borden KL, Boddy MN, Freemont PS. Does this have a familiar RING? *Trends Biochem Sci.* 1996;21(6):208-214.
24. Zhang XW, Yan XJ, Zhou ZR, et al. Arsenic trioxide controls the fate of the PML-RARalpha oncoprotein by directly binding PML. *Science.* 2010;328(5975):240-243.
25. Jeanne M, Lallemand-Breitenbach V, Ferhi O, et al. PML/RARA oxidation and arsenic binding initiate the antileukemia response of As2O3. *Cancer Cell.* 2010;18(1):88-98.
26. Atsumi A, Tomita A, Kiyoi H, Naoe T. Histone deacetylase 3 (HDAC3) is recruited to target promoters by PML-RARalpha as a component of the N-CoR co-repressor complex to repress transcription in vivo. *Biochem Biophys Res Commun.* 2006;345(4):1471-1480.
27. Hiraga J, Tomita A, Sugimoto T, et al. Down-regulation of CD20 expression in B-cell lymphoma cells after treatment with rituximab-containing combination chemotherapies: its prevalence and clinical significance. *Blood.* 2009;113(20):4885-4893.
28. Tomita A, Buchholz DR, Obata K, Shi YB. Fusion protein of retinoic acid receptor alpha with promyelocytic leukemia protein or promyelocytic leukemia zinc finger protein recruits N-CoR-TBLR1 corepressor complex to repress transcription in vivo. *J Biol Chem.* 2003;278(33):30788-30795.
29. Tomita A, Buchholz DR, Shi YB. Recruitment of N-CoR/SMRT-TBLR1 corepressor complex by unliganded thyroid hormone receptor for gene repression during frog development. *Mol Cell Biol.* 2004;24(8):3337-3346.
30. Hayakawa F, Privalsky ML. Phosphorylation of PML by mitogen-activated protein kinases plays a key role in arsenic trioxide-mediated apoptosis. *Cancer Cell.* 2004;5(4):389-401.
31. Golomb HM, Rowley JD, Vardiman JW, Testa JR, Butler A. "Microgranular" acute promyelocytic leukemia: a distinct clinical, ultrastructural, and cytogenetic entity. *Blood.* 1980;55(2):253-259.
32. Pandolfi PP, Alcalay M, Fagioli M, et al. Genomic variability and alternative splicing generate multiple PML/RAR alpha transcripts that encode aberrant PML proteins and PML/RAR alpha isoforms in acute promyelocytic leukaemia. *EMBO J.* 1992;11(4):1397-1407.
33. Lallemand-Breitenbach V, Jeanne M, Benhenda S, et al. Arsenic degrades PML or PML-RARalpha through a SUMO-triggered RNF4/ubiquitin-mediated pathway. *Nat Cell Biol.* 2008;10(5):547-555.
34. Borden KL, Lally JM, Martin SR, O'Reilly NJ, Solomon E, Freemont PS. In vivo and in vitro characterization of the B1 and B2 zinc-binding domains from the acute promyelocytic leukemia protooncoprotein PML. *Proc Natl Acad Sci U S A.* 1996;93(4):1601-1606.
35. Flenghi L, Fagioli M, Tomassoni L, et al. Characterization of a new monoclonal antibody (PG-M3) directed against the aminoterminal portion of the PML gene product: immunocytochemical evidence for high expression of PML proteins on activated macrophages, endothelial cells, and epithelia. *Blood.* 1995;85(7):1871-1880.
36. Fagioli M, Alcalay M, Tomassoni L, et al. Cooperation between the RING + B1-B2 and coiled-coil domains of PML is necessary for its effects

on cell survival. *Oncogene.* 1998;16(22):2905-2913.

37. Huang W, Sun GL, Li XS, et al. Acute promyelocytic leukemia: clinical relevance of two major PML-RAR alpha isoforms and detection of minimal residual disease by retrotranscriptase/polymerase chain reaction to predict relapse. *Blood.* 1993;82(4):1264-1269.
38. Vahdat L, Maslak P, Miller WH Jr, et al. Early mortality and the retinoic acid syndrome in acute promyelocytic leukemia: impact of leukocytosis, low-dose chemotherapy, PMN/RAR-alpha isoform, and CD13 expression in patients treated with all-trans retinoic acid. *Blood.* 1994;84(11):3843-3849.
39. Ishov AM, Sotnikov AG, Negorev D, et al. PML is critical for ND10 formation and recruits the PML-interacting protein daxx to this nuclear structure when modified by SUMO-1. *J Cell Biol.* 1999;147(2):221-234.
40. Lallemand-Breitenbach V, de The H. PML nuclear bodies. *Cold Spring Harb Perspect Biol.* 2010;2(5):a000661.
41. Zhou DC, Kim SH, Ding W, Schultz C, Warrell RP Jr, Gallagher RE. Frequent mutations in the ligand-binding domain of PML-RARalpha after multiple relapses of acute promyelocytic leukemia: analysis for functional relationship to response to all-trans retinoic acid and histone deacetylase inhibitors in vitro and in vivo. *Blood.* 2002;99(4):1356-1363.
42. Côté S, Zhou D, Bianchini A, Nervi C, Gallagher RE, Miller WH Jr. Altered ligand binding and transcriptional regulation by mutations in the PML/RARalpha ligand-binding domain arising in retinoic acid-resistant patients with acute promyelocytic leukemia. *Blood.* 2000;96(9):3200-3208.
43. Ding W, Li YP, Nobile LM, et al. Leukemic cellular retinoic acid resistance and missense mutations in the PML-RARalpha fusion gene after relapse of acute promyelocytic leukemia from treatment with all-trans retinoic acid and intensive chemotherapy. *Blood.* 1998;92(4):1172-1183.
44. Imaizumi M, Suzuki H, Yoshinari M, et al. Mutations in the E-domain of RAR portion of the PML/RAR chimeric gene may confer clinical resistance to all-trans retinoic acid in acute promyelocytic leukemia. *Blood.* 1998;92(2):374-382.
45. Marasca R, Zucchini P, Galimberti S, et al. Missense mutations in the PML/RARalpha ligand binding domain in ATRA-resistant As(2)O(3) sensitive relapsed acute promyelocytic leukemia. *Haematologica.* 1999;84(11):963-968.
46. Lin RJ, Nagy L, Inoue S, Shao W, Miller WH Jr, Evans RM. Role of the histone deacetylase complex in acute promyelocytic leukaemia. *Nature.* 1998;391(6669):811-814.
47. Grignani F, De Matteis S, Nervi C, et al. Fusion proteins of the retinoic acid receptor-alpha recruit histone deacetylase in promyelocytic leukaemia. *Nature.* 1998;391(6669):815-818.
48. Zhu Q, Zhang JW, Zhu HQ, et al. Synergic effects of arsenic trioxide and cAMP during acute promyelocytic leukemia cell maturation subtends a novel signaling cross-talk. *Blood.* 2002;99(3):1014-1022.
49. Zhou J, Zhang Y, Li J, et al. Single-agent arsenic trioxide in the treatment of children with newly diagnosed acute promyelocytic leukemia. *Blood.* 2010;115(9):1697-1702.

Cell Stem Cell
Article

TIM-3 Is a Promising Target to Selectively Kill Acute Myeloid Leukemia Stem Cells

Yoshikane Kikushige,[1] Takahiro Shima,[1] Shin-ichiro Takayanagi,[2] Shingo Urata,[1] Toshihiro Miyamoto,[1] Hiromi Iwasaki,[1] Katsuto Takenaka,[1] Takanori Teshima,[1] Toshiyuki Tanaka,[3] Yoshimasa Inagaki,[2] and Koichi Akashi[1,*]
[1]Department of Medicine and Biosystemic Sciences, Kyushu University Graduate School of Medicine, Fukuoka 812-8582, Japan
[2]Innovative Drug Research Laboratories Kyowa Hakko Kirin Co., Ltd., Tokyo 194-8538, Japan
[3]School of Pharmacy, Hyogo University of Health Sciences, Kobe 650-8530, Japan
*Correspondence: akashi@med.kyushu-u.ac.jp
DOI 10.1016/j.stem.2010.11.014

SUMMARY

Acute myeloid leukemia (AML) originates from self-renewing leukemic stem cells (LSCs), an ultimate therapeutic target for AML. Here we identified T cell immunoglobulin mucin-3 (TIM-3) as a surface molecule expressed on LSCs in most types of AML except for acute promyelocytic leukemia, but not on normal hematopoietic stem cells (HSCs). TIM-3$^+$ but not TIM-3$^-$ AML cells reconstituted human AML in immunodeficient mice, suggesting that the TIM-3$^+$ population contains most, if not all, of functional LSCs. We established an anti-human TIM-3 mouse IgG2a antibody having complement-dependent and antibody-dependent cellular cytotoxic activities. This antibody did not harm reconstitution of normal human HSCs, but blocked engraftment of AML after xenotransplantation. Furthermore, when it is administered into mice grafted with human AML, this treatment dramatically diminished their leukemic burden and eliminated LSCs capable of reconstituting human AML in secondary recipients. These data suggest that TIM-3 is one of the promising targets to eradicate AML LSCs.

INTRODUCTION

Acute myeloid leukemia (AML) is a clonal malignant disorder derived from a small number of leukemic stem cells (LSCs). LSCs self renew and generate leukemic progenitors that actively divide to produce a large number of immature clonogenic leukemic blasts (Bonnet and Dick, 1997; Hope et al., 2004; Lapidot et al., 1994). This hierarchical stem cell-progenitor-mature cell relationships in AML appears to simulate normal hematopoiesis that originates from hematopoietic stem cells (HSCs) with self-renewal activity. We have shown that like normal HSCs, AML LSCs are quiescent in vivo and appear to reside at the endosteal "osteoblastic" niche in the bone marrow based on our analysis in a xenograft model (Ishikawa et al., 2007). AML LSCs are resistant to chemotherapeutic reagents that usually target cycling malignant cells. In the majority (~90%) of AML patients, the conventional chemotherapies can diminish the leukemic clones to achieve remission. However, ~60% of such remission patients still relapse, and the recurrence of AML in these patients should originate from LSCs that survive the intensive chemotherapies. Therefore, the LSC should be the ultimate cellular target to cure human AML.

To eradicate the AML LSC without killing normal HSCs, it is critical to isolate a molecule that is expressed or functions specifically at the AML LSC stage (Krause and Van Etten, 2007). It has been shown that the AML LSCs mainly reside within the CD34$^+$CD38$^-$ fraction of leukemic cells and can reconstitute human AML in immunodeficient mice (Lapidot et al., 1994), although recent studies have suggested that LSCs can exist also in CD34$^+$CD38$^+$ (Taussig et al., 2008) or CD34$^-$ blastic fractions at least in some types of AML (Martelli et al., 2010; Taussig et al., 2010). Normal HSCs with long-term reconstitution activity also have the CD34$^+$CD38$^-$ phenotype (Bhatia et al., 1997; Ishikawa et al., 2005). However, the expression pattern of other surface molecules in the CD34$^+$CD38$^-$ fraction of AML cells is different from that of normal controls. For example, CD34$^+$CD38$^-$ AML cells possess many phenotypic characteristics analogous to normal granulocyte/macrophage progenitors (GMPs) (Yoshimoto et al., 2009). Previous studies have reported molecules preferentially expressed in AML cells. Such molecules include CLL-1 (van Rhenen et al., 2007), CD25, CD32 (Saito et al., 2010), CD33 (Florian et al., 2006; Hauswirth et al., 2007), CD44 (Florian et al., 2006; Jin et al., 2006), CD47 (Jaiswal et al., 2009; Majeti et al., 2009), CD96 (Hosen et al., 2007), and CD123 (Jin et al., 2009; Yalcintepe et al., 2006). However, in our hands, some of these molecules are expressed in LSCs at a level insufficient for clear distinction, are expressed also in normal HSCs at a considerable level, or are found only in a fraction of AML cases. It is therefore critical to isolate ideal targets for AML LSCs with sufficient specificity and sensitivity.

Here we report a new surface molecule that might be useful to eradicate AML LSCs leaving normal HSC intact. We performed differential transcriptional profiling of AML LSCs and HSCs and extracted the T cell immunoglobulin mucin-3 (TIM-3) as a promising AML LSC-specific target surface molecule. TIM-3 is originally found as a surface molecule expressed in CD4$^+$ Th1 lymphocytes in mouse hematopoiesis and is an important regulator of Th1 cell immunity and tolerance induction (Monney et al., 2002; Sabatos et al., 2003; Sánchez-Fueyo et al., 2003). Murine TIM-3 is also expressed in CD11b$^+$ macrophages and CD11c$^+$ dendritic cells and recognizes apoptotic cells' phosphatidylserine through its IgV domain to mediate phagocytosis (Nakayama et al., 2009).

We found that human TIM-3 was expressed in the vast majority of CD34$^+$CD38$^-$ LSCs and CD34$^+$CD38$^+$ leukemic progenitors in AML of most FAB types, except for acute

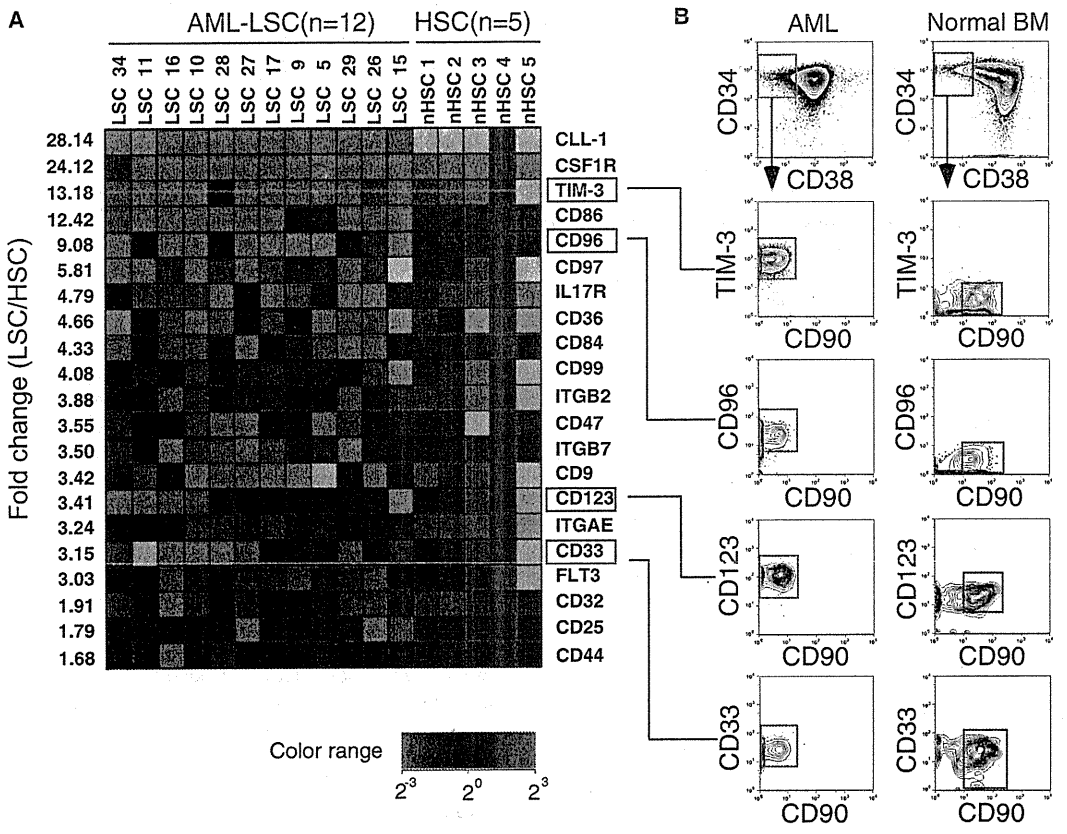

Figure 1. The Expression of LSC-Specific Surface Molecules in AML

The $CD34^+CD38^-$ adult bone marrow HSCs and $CD34^+CD38^-$ AML LSCs were purified and tested for their surface molecule expression.

(A) Results of cDNA microarray analysis of HSCs and AML LSCs. Representative genes coding surface molecules that are expressed highly in AML LSCs are shown. TIM-3 is expressed specifically in LSCs at high levels in the majority of AML patients. Patient numbers correspond to those in Table S1.

(B) The expression of representative surface proteins in HSCs and AML LSCs on FACS.

promyelocytic leukemia (M3). TIM-3 was not expressed in $CD34^+CD38^-$ normal HSCs or the vast majority of $CD34^+$ $CD38^+$ normal progenitors. Administration of anti-human TIM-3 mouse antibodies with a complement-dependent cytotoxicity (CDC) and an antibody-dependent cellular cytotoxicity (ADCC) selectively inhibited engraftment and development of human AML in xenograft models. Our data strongly suggest that the use of TIM-3 to target AML LSCs is a promising approach for the improvement of leukemia therapy.

RESULTS

TIM-3 Is Expressed in the $CD34^+CD38^-$ Fraction of AML Patients' Bone Marrow Cells

In most types of AML, LSCs are concentrated in the $CD34^+$ $CD38^-$ fraction of AML cells (Ishikawa et al., 2007; Lapidot et al., 1994), whose phenotype is common to normal adult HSCs. Patients' characteristics are shown in Table S1 available online. To search for the AML LSC-specific molecules, 10,000 each of purified $CD34^+CD38^-$ AML cells and $CD34^+CD38^-$ normal HSCs were subjected to cDNA microarray analysis. We extracted 256 genes with >4-fold change between normal HSCs and $CD34^+CD38^-$ AML cells and then selected 197 differentially expressed genes with <0.01 of a cut-off p value (Table S2). Genes coding surface molecules that are expressed highly in $CD34^+CD38^-$ AML cells were selected for this study. Figure 1A shows the mRNA levels of candidate LSC-specific surface molecules in purified $CD34^+CD38^-$ AML cells and normal HSCs. The molecules expressed in $CD34^+CD38^-$ AML cells at levels >8-fold higher as compared to normal HSCs included TIM-3 and previously identified LSC-specific molecules such as CLL-1 (van Rhenen et al., 2007), CSF1R (Aikawa et al., 2010), and CD96 (Figure 1A; Hosen et al., 2007). As shown in Figure 1B, TIM-3 protein was highly expressed in $CD34^+CD38^-$ AML cells but not in normal HSCs. We focused on TIM-3 not only because it is expressed specifically in $CD34^+CD38^-$ AML cells at high levels, but also because it is expressed in the majority of patients with most AML types.

We evaluated the TIM-3 protein expression on cell surface of AML cells by FACS analysis. As shown in Figure 2, the vast majority of the $CD34^+CD38^-$ LSCs as well as $CD34^+CD38^+$ progenitor fractions in AML M0, M1, M2, and M4 types expressed TIM-3 at a high level in virtually all cases studied. In AML M5, M6, and M7, a considerable fraction of $CD34^+CD38^-$ cells

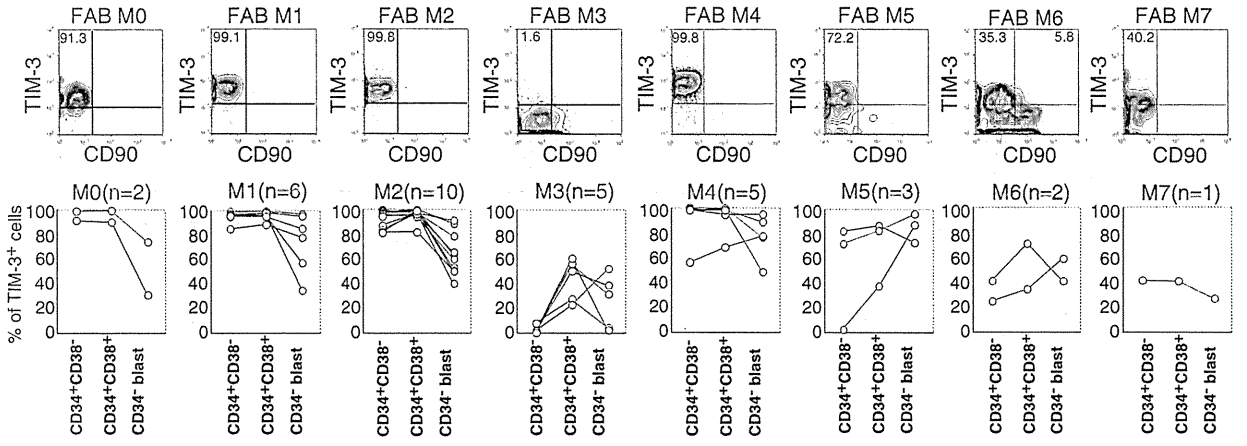

Figure 2. The Expression of TIM-3 in Stem and Progenitor Populations of AML of Each FAB Type
Expression of TIM-3 in each FAB type of AML. The representative expression pattern of TIM-3 in the $CD34^+CD38^-$ LSC fraction (top) and distribution of TIM-3 in $CD34^+CD38^-$ LSCs, $CD34^+CD38^+$ leukemic progenitors, and $CD34^-$ leukemic blasts (bottom) are shown.

expressed TIM-3. TIM-3 was, however, not expressed in the $CD34^+CD38^-$ population in all five M3 cases tested. In general, TIM-3 was expressed in both $CD34^+CD38^-$ LSCs and $CD34^+CD38^+$ leukemic progenitor fractions, but its expression tended to decline at the $CD34^-$ leukemic blast stage (Figure 2, bottom).

The TIM-3-Expressing of AML Fraction Contains the Vast Majority of Functional LSCs in a Xenograft Model

Recent studies have suggested that at least in some AML cases, LSCs that are capable of initiating human AML in xenograft models reside not only within the $CD34^+CD38^-$ fraction but also outside of this population including $CD34^+CD38^+$ (Taussig et al., 2008) or $CD34^-$ (Martelli et al., 2010; Taussig et al., 2010) AML cells. To evaluate whether functional AML LSCs express TIM-3, 10^6 cells of human TIM-3^+ and TIM-3^- AML populations were transplanted into sublethally irradiated immunodeficient mice. We used NOD.Cg-*Rag1*^{tm1Mom} *Il2rg*^{tm1Wjl}/SzJ (NRG) mice for the xenogeneic transplantation experiments, by which higher chimerism of human hematopoietic cells was observed in xenotransplantation assays (Pearson et al., 2008). Recipients transplanted with TIM-3^+ and TIM-3^- AML cells were sacrificed 8–10 weeks after transplantation. As shown in Figure 3, human $CD45^+CD33^+$ AML cells were

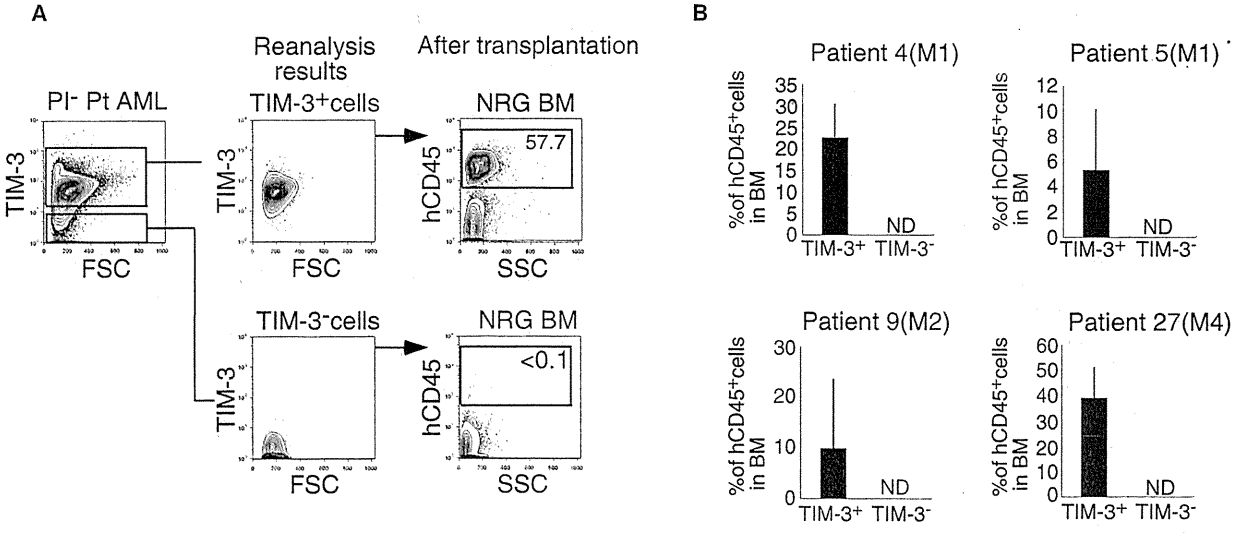

Figure 3. The TIM-3^+ AML Population Contains the Vast Majority of Functional LSC Activity
(A) A representative analysis of xenotransplantation of purified TIM-3^+ or TIM-3^- AML cells from patient 27 into NRG mice. Only TIM-3^+ cells reconstitute $hCD45^+$ AML cells after transplantation.
(B) Summarized data of four independent experiments. Only TIM-3^+ (not TIM-3^-) AML cells reconstituted human AML cells in xenotransplantation experiments in all experiments, suggesting that most functional LSCs reside in the TIM-3^+ AML fraction.